BOEING

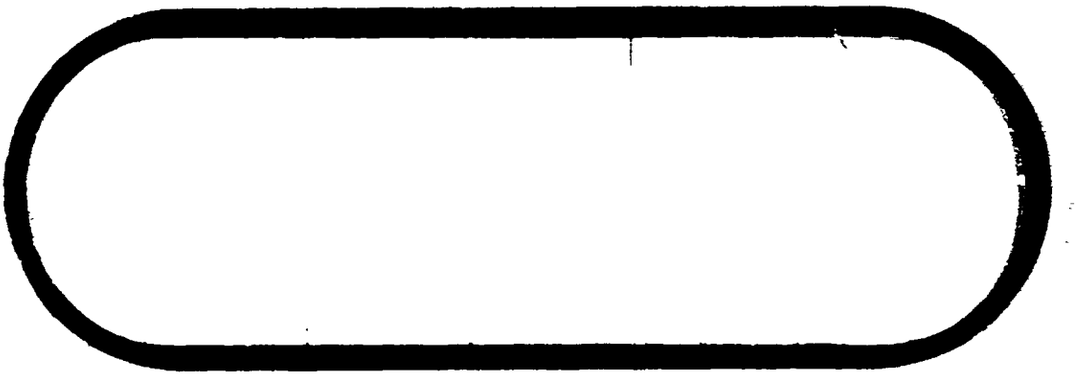

D256-10024

FURTHER ANALYSIS OF FIELD EFFECTS ON LIQUIDS AND SOLIDIFICATION

FINAL REPORT
CONTRACT NAS8-28664 (MOD I)
(1-3-50-32690 1F)

STUDY OF THE LIQUID-SOLID TRANSITION
FOR
MATERIALS PROCESSING IN SPACE
JULY 9, 1974

PREPARED BY
THE NUCLEAR AND SPACE PHYSICS GROUP
BOEING AEROSPACE COMPANY
P.O. BOX 1470
HUNTSVILLE, ALABAMA 35807

R.F.SEILER - PROGRAM MANAGER
R. I. MILLER - PRINCIPAL INVESTIGATOR
W.S.CHEN - MATERIALS SPECIALIST

PREPARED FOR

NATIONAL AERONAUTICS AND SPACE ADMINISTRATION
GEORGE C. MARSHALL SPACE FLIGHT CENTER
MARSHALL SPACE FLIGHT CENTER, ALABAMA

TABLE OF CONTENTS

TABLE OF CONTENTS (Continued)

LIST OF FIGURES

LIST OF FIGURES (Continued)

LIST OF TABLES

LIST OF SYMBOLS

A	- $k\, T_M \Gamma\, V'V / m\, G_c D^2$
a	- cylinder radius - algebraic constant to be determined
$\vec{B}$ (B)	- magnetic induction field (magnitude of $\vec{B}$)
B.P.	- boiling point
b	- cylinder radius - algebraic constant to be determined
C	- solute concentration
C_0	- solute concentration at a planar interface
C_∞	- $C(x,\infty) = C_0\, k\, \frac{V}{V'}$
$c_{P,S,L}$	- specific heat at constant pressure, of solid, of liquid
D	- diffusion coefficient
D_{th}	- thermal diffusivity of a liquid
D'_{th}	- thermal diffusivity of a solid
e	- base of natural logarithms, 2.71828 .... - charge of an electron, 1.6 X 10^{-19} coulomb
$\vec{F}$	- force
$\vec{f}$ (f)	- body force (magnitude of $\vec{f}$)
f_e	- eddy current body force
f_g	- gravitational body force
f_m	- magnetic body force
$\vec{f}$ (a)	- random spacecraft acceleration function

LIST OF SYMBOLS (Continued)

$\hat{G}$	- universal gravitation constant
	- thermal gradient in a liquid
G_c	- concentration gradient
G'	- thermal gradient in a solid
$\underline{G}$, $\underline{G}'$	- see page 2-46
ΔG	- Gibbs free energy of solidification
$\vec{g}$ (g)	- acceleration due to earth's gravity (magnitude of $\vec{g}$)
$\vec{H}$ (H)	- magnetic field strength (magnitude of $\vec{H}$)
H_0	- magnetic field in a material-free region
H_f	- enthalpy of fusion
h	- Hartmann number
$\hat{i}$	- unit vector in x direction
$\vec{J}$ (J)	- current density (magnitude of $\vec{J}$)
$\vec{J}_e$	- eddy current density
$J(\frac{G}{V},\frac{V}{V'},C_\infty)$	- see page 2-53
$\hat{j}$	- unit vector in y direction
K_L (K_S)	- thermal conductivity of a liquid (solid)
$\overline{K}$	- see page 2-46
$\hat{K}$	- unit vector in z direction
k	- Boltzmann's constant, $1.3804 \times 10^{-16} \frac{erg}{deg}$
	- segregation coefficient, C_S/C_L
k'	- $k\frac{V}{V'}$

LIST OF SYMBOLS (Continued)

L	- characteristic length
	- Lorentz number
$\hat{M}$	- magnetization
m	- molecular mass
	- slope of liquidus curve on phase diagram
$\vec{m}_i$	- molecule (atom) magnetic moment
N_0	- Avogadro's number, 6.025×10^{23} mole^{-1}
$\hat{n}$	- unit vector normal to a surface
P	- pressure
ΔP	- pressure change
p	- 1-k
Q	- heat of fusion
R	- Hall coefficient
r	- $(1+\theta y_m)^{1/4}$
	- radial coordinate
$\hat{r}$	- unit vector in r direction
S	- 1 - [minimum Y(y)], stability function
S_c	- entropy of solidification
S_f	- entropy of melting
$d\vec{s}$	- differential element of surface area vector

LIST OF SYMBOLS (Continued)

T	- absolute temperature (Kelvin)
T_m	- melting temperature
TEP	- thermoelectric power
ΔT	- temperature change
δT	- undercooling
t	- time
U_c	- solidification rate
$\vec{u}$ (u)	- velocity (magnitude of $\vec{u}$)
$\bar{u}$	- gas kinetic velocity
V	- total volume - velocity of planar liquid - solid interface
V'	- V-u
v	- specific volume
v_f	- free volume
v^*	- Free Volume Model critical volume
v_0	- molecular volume
dv	- differential volume element
Δv	- volume change
X	- unknown quantity symbol
x	- coordinate
$Y(y)$	- $\frac{2k'}{y+(1+\theta y)^{1/2}-1+2k'}$

LIST OF SYMBOLS (Continued)

y	- coordinate - $\frac{T_m \Gamma \omega^2}{mG_c}$
y_m	- value of y minimizing Y(y)
Z	- atomic number
z	- axial coordinate or vertical distance
α	- thermal expansion coefficient
β	- isothermal compressibility
Γ	- capillary constant, γ/Q
γ	- liquid-solid interface free energy - Free Volume Model overlap factor
$\delta(t)$	- interface perturbation amplitude
$\dot{\delta}$	- $d\delta/dt$
ϵ	- Lennard-Jones energy parameter
η	- molecular viscosity
η_m	- magnetic viscosity
θ	- $4k'/A$ - azimuthal angle coordinate
$\hat{\theta}$	- unit vector in θ direction ($\perp \hat{r}$)

LIST OF SYMBOLS (Continued)

κ	- thermal conductivity - liquid-solid interface curvature
λ	- interface perturbation wavelergth (concentration cell size)
μ	- permeability
μ_0	- permeability of free space
ν	- kinematic viscosity - mobility
ρ	- density
ρ_e	- electrical resistivity
σ	- electrical conductivity - surface tension - Lennard-Jones molecular separation constant
τ	- time constant
ϕ	- Lennard-Jones potential function - magnetic field potential - interface shape function
χ	- magnetic susceptibility
ψ	- Free Volume Model parameter - gravitational potential

LIST OF SYMBOLS (Continued)

ω	- $2\pi/\lambda$
ω_m	- maximum value of ω
$\omega^*, \omega_{th}, \omega'_{th}$	- see page 2-46
$\vec{\nabla}$	- gradient vector operator
∇^2	- Laplacian operator

SECTION I

SUMMARY

Objectives

The objectives of the first contract "Study of the Liquid-Solid Transition for Materials Processing in Space" have been discussed in Reference 1, and these objectives continue to apply to the second year's effort (Modification 1) which is described in this report. The objectives are:

1. To analyze the behavior of dense liquids near the solidification point while the liquid in question is under the influence of magnetic fields or near-zero gravity conditions, and

2. to do this within the framework of existing liquid state models and classical field theory.

In the present work, these objectives have been extended to include numerical calculation of the magnitudes of external field effects on liquids and to describe how external fields can influence the substructure of the solid during the solidification process. The materials considered in this analysis are (as much as possible) semiconducto s and metals, since these are the materials of most interest in the Space Processing Program.

Approach

The approach employed for this second year of the Liquid-Solid Transition Study was to build on the knowledge of liquid state models and field-liquid interactions gained during the first year. This was done by defining three tasks and several subtasks:

Task 1 - Liquid Property Data Search

Task 2 - Determination of Field Effects on Solute Distribution

- 2A - Analysis of Field Distributions in Melts
- 2B - Calculation of Field Forces on Solute Atoms and Resultant Velocities
- 2C - Relation of Microsegregation to Solute Atom Velocity

Task 3 - Analysis of Field Effects on Liquids

- 3A - Calculation of Magnetoviscous Effects
- 3B - Calculation of Field Effects on Diffusion and Related Phenomena
- 3C - Analysis of Body Forces Due to Oscillating Magnetic Fields

The experimental values of basic liquid properties obtained in Task 1 were used in Task 3 as input to the theoretical equations derived in Reference 1. Calculations performed in Task 3 then provide quantitative estimates of the effects which magnetic and gravitational fields have on melts of metals or semiconductors. Task 2 was essentially a new effort to develop a model of the solidification process which would describe to some extent the effects external fields will produce on the substructure of the solid.

The qualitative analysis performed during the initial year of the study suggested approaches for further investigation and calculation in several areas. The magnetodynamic effects of interest included the magnitude of the induced magnetic viscosity and its importance relative to the molecular viscosity as measured by the Hartmann number. Analysis of radio-frequency (R-F) field effects can easily be generalized to any oscillating magnetic field since all time-varying magnetic fields induce eddy currents in conducting media. These eddy currents then

interact with the magnetic field to produce body forces on melts of metals or semiconductors placed in an oscillating magnetic field. In order to obtain a quantitative feeling for these eddy current body forces, they are compared to both the viscous force induced by the field and to the gravitational body force, ρg, as described in Section 2.2. External field effects on diffusive phenomena were approached through the Free Volume Model descriptions of diffusion coefficient and solidification rate. This approach describes only the direct effects fields have on these and related quantities, and neglects any effects of convection which are considered to some extent in Section 2.2. The Task 2 description of how external fields affect solute segregation during solidification was approached through a four step procedure which (1) relates the field distribution inside a melt to the external field inducing it, (2) calculates the force on a solute atom due to the internal field, (3) relates solute atom velocity in the melt to the driving force found in step (2), and (4) uses Sekerka's stability theory to show how solute atom velocity in the melt influences solute microsegregation in the solid. Thus emphasis was placed on development of procedures for doing practical calculations of solidification parameters affected by external fields (in Task 3) and on development of a mathematical model which formally describes field effects on microsegregation (in Task 2).

Results

The search for experimental values of liquid property data has identified 39 papers (Table I) and 12 books (Table II) containing data useful in the study of external field effects on melts of semiconductors or metals. Additional references dealing with liquid state theory and problems are given in Section 2.5, and each of these references themselves contain references to works dealing with other problems or data pertinent to the study of real liquids and liquid state models. The results of the data search which apply to the investigation of field effects on solidification are condensed in Tables III and V which

contain the input data for calculation of magnetic and gravitational field effects on diffusion coefficient, solidification rate and for calculation of field forces on individual molecules in the melt. There are two reasons why data for more than four materials does not appear in Table III. First, there has been very little experimental work done on liquid metals and semiconductors as compared to solids, gases and organic liquids, and so there is a dearth of experimental data for the physical properties of these materials. Second, for a given material, one must find some eleven material properties just to do the calculations required for the diffusion coefficients and solidification rates. The materials listed in Table III were the only liquids for which values of all eleven properties could be found simultaneously.

Calculations of magnetic viscosity and Hartmann number show that magnetoviscous effects predominate in the metals and semiconductors studied for fields on the order of about 10 gauss or above. This is in agreement with the finding that gravity-driven convection velocity decays exponentially with a time constant inversely proportional to the square of the magnetic induction field applied to the melt to induce the magnetic viscosity. Eddy current body forces induced in melts by oscillating magnetic fields are quadratic functions of field strength. Because the susceptibilities of most paramagnetic and diamagnetic liquids are on the order of 10^{-6} cgs units, the values of the eddy current body force (f_e) for any of these liquids at a fixed field strength are equal within 0.001%. Comparison of f_e to other forces on the melt shows that eddy current forces usually predominate, even over the magnetoviscous force, which arises from the same field as f_e. This predominance depends, however, on the value of $\vec{u}$, the initial convection velocity, in the magnetic viscosity case, and on the ratio $\frac{H^2}{\rho}$ in the comparison of f_e to gravitational body forces, where H is magnetic field strength and ρ is liquid density.

Turnbull's Free Volume Model of the liquid state and the liquid-solid transition was used to calculate direct effects of external fields on diffusion coefficients and solidification rates of selected representative materials. Direct effects are those derivable directly from the fields and not attributable to convective or magnetohydrodynamic effects. The results of this analysis indicate that microgravity causes infinitesimal changes (10^{-5}% - 10^{-6}%) in diffusion coefficient and solidification rates while the changes caused by a magnetic field of 10^5 oersteds are small (0.3% - 1.9%) but finite. Changes in diffusion coefficient or solidification rate in a magnetic field are dependent on the square of the field strength, and thus vary widely with field strength. The diffusion coefficient was found to increase in microgravity over its value on Earth, while whether it increases or decreases in a magnetic field depends on several parameters, primarily the field strength. The free energy term (see equation 14) decreases for all materials considered in microgravity, and its change in a magnetic field is dependent on the sign of the susceptibility difference, $\chi_\ell - \chi_s$, and on the ratio of the free energy in zero field to the heat of fusion. Changes in solidification rate are, from equation (14), dependent on the relative magnitudes of the free energy term change and diffusion coefficient change. In the examples chosen, the solidification rate decreased in microgravity and increased in a magnetic field of 10^5 oersteds.

It should be noted here that Wang computer programs have been written for calculation of the following parameters:

Eddy current body force
Ratio of eddy current force to gravitational body force
D'/D (magnetic field case)
Free energy term (magnetic field case)
Isothermal compressibility
Coefficient of thermal expansion
Entropy
Specific heat at constant pressure

Free Volume Model a^2 parameter
Conversion of density to specific volume.

In Task 2 of the present contract, a model has been developed which formally relates external fields to solute distribution in solids. The existence of such a formal relationship constitutes a significant result, but the model in its present form is severely limited in its range of applicability and accuracy. The major limitations are as follows:

(a) Exact, analytical solutions for magnetic field distributions satisfying the boundary conditions on melts for Czochralski crystal growth geometry cannot be obtained,

(b) Random acceleration (gravity) fields in orbiting spacecraft are not well known,

(c) Intermolecular forces in liquids are not well understood, and the problem of describing the effects of more than one field acting simultaneously on a molecule in a liquid requires more study,

(d) Sekerka's theory of interface stability is capable of estimating segregation cell size to only an order of magnitude because the theory is based on the small perturbation approximation, and

(e) Analysis of cases in which solute molecule velocity is in any direction other than that of the solidification velocity is extremely difficult and will require much more research.

Results obtained under the above limitations include the determination of the occurrence of microsegregation as a function of the parameters $V - \frac{u}{p}$ where V is macroscopic solidification velocity, u is solute molecule velocity and $p = 1-k$ with k being the segregation coefficient

for the material considered, and estimates of the size of cells of different solute concentration values in the solid.

During the years this contract has been active, work performed under the contract has resulted in seven scientific publications (two already published in international journals) and four presentations to scientific meetings (one invited). These are listed in Appendix A.

Conclusions and Recommendations

The major conclusions of this study are:

1. Values of the physical properties of molten semiconductors are difficult to obtain from the literature because very little experimental research has been done in this area,

2. Of the research on liquid semiconductor properties which has been reported, much of it has been done by Russian researchers,

3. Moderate and high magnetic fields produce strong forces in melts and damp out convective flows exponentially,

4. Oscillating magnetic fields induce body forces even stronger than the static field magnetoviscous force,

5. The direct effects of microgravity on melts of the materials considered in this study were infinitesimal, while the effects of magnetic fields were dependent on field strength and were small but finite,

6. The lack of a large direct effect of microgravity on liquids supports the thesis that the primary benefits of materials processing in space arise from secondary effects, such as the suppression of convection or the reduction of contamination by containerless processing,

7. A formal relationship between external fields and solute distribution in a solid during solidification has been established,

8. The occurrence of microsegregation depends on the parameters $(V - \frac{u}{p})$ and ω, where ω is related to the interface perturbation or cell size,

9. There are several practical limitations to the theory which describes microsegregation dependence on external fields, including

   - the difficulty of obtaining gravitational (acceleration) field distributions in melts aboard an orbital laboratory or magnetic field distributions in melts during Czochralski growth on Earth,
   - the difficulty of representing the process of several fields acting on a molecule at once, and
   - the failure of the small perturbation approximation (which linearizes the temperature and concentration field equations) to yield results which agree well with experiment.

Thus it is seen that, for the materials for which experimental property data are available, the similarity of microgravity and magnetic field effects on melts holds only for very low magnetic fields, and the effects are quantitatively quite different at higher magnetic field strengths. This was to be expected, since the magnetic interaction is much stronger than gravity, and has now been verified.

The relationship of microsegregation in solids to external fields applied during solidification is found to be very complicated and not well understood at present. It is recommended that much more research be done in this area, specifically in

- representing field distributions in melts,
- defining resulting forces on individual molecules and deriving the corresponding velocities, and
- overcoming the limitations of the small perturbation approximation in calculating segregation cell sizes when microsegregation occurs.

It is further recommended that research begin on a flight experiment whose objective would be to compare the theory of Section 2.4 to experimental measurements of interface stability in a convection-free environment where the small perturbation approximation may be valid.

SECTION 2

ANALYTICAL RESULTS

2.1 LIQUID STATE PROPERTY DATA SEARCH

The work detailed in Reference 1 provides a qualitative theoretical description of many effects which magnetic and gravitational fields produce on melts during solidification processes, but there are two reasons why it is desirable to obtain a quantitative understanding of these effects. First, in most cases, the equations describing the field effects of interest do not give an obvious indication of the magnitude or direction of the change in liquid properties due to the field change without actually performing the calculations defined by the equations. Second, it is always helpful in understanding physical phenomena described by equations to become familiar with the numerical value of the various parameters in the equations as they correspond to different materials or conditions. For these reasons it was decided to perform numerical calculations of the field effects derived in Reference 1, and to do this, it was necessary to obtain numerical values of all parameters appearing in the equations describing the effects.

These experimental values were to be obtained for materials similar to those most prominent in the Space Processing Program, i.e., those which show promise of improvement in their economically beneficial properties when processed in space. Semiconductors and metals, and in particular, Group III - Group V compounds were the materials receiving the most attention in the Space Processing discipline at the beginning of the contract, thus the search for experimental data centered on these types of materials. The search encompassed a computer search of NASA and DOL data banks, searches of the Physics Abstracts, the Science Citation Index, the Redstone Scientific Information Center book collection and personal contacts with experimental researchers at universities and other companies. It was found that

2.1 (Continued)

much of the property data for molten semiconductors has been measured by Russian researchers, and that most of the Russian work deals with electrical properties of melts other than III-V compounds. Data for the III-V compounds corresponding to parameters and properties in the field effect equations[1] proved extremely difficult, and in many cases impossible, to find. Tables I and II list references for the journal articles and books containing liquid property data which were identified in the search. The tables also indicate the particular materials and properties considered by each reference. It must be noted that each reference shown in these tables also contains references to other works on liquid metals or semiconductors, therefore these lists of references are intended as a starting point for researchers interested in a variety of materials and properties. Sufficient data was found for indium antimonide (InSb), germanium (Ge), mercury (Hg) and sodium (Na) to allow calculation of external field effects on temperature, volume, Gibbs free energy, diffusion coefficient and solidification rate as will be described in Section 2.3 (see Table III).

2.2 MAGNETODYNAMIC EFFECTS ON MELTS

Several macroscopic dynamic effects which are produced by magnetic fields are worthy of understanding in their own right and also may be helpful in understanding microgravity effects on melts.

Calculations of Magnetic Viscosity and Hartmann Number

Previous work has shown[1] that the magnetic viscosity induced in a melt with electrical conductivity σ is related to the magnetic induction $\vec{B}$ by

$$\eta_m = \sigma B^2 L^2 \qquad (1)$$

2.2 (Continued)

TABLE I

LIQUID STATE PHYSICAL PROPERTIES REFERENCE LIST

	REFERENCE	DATE	MATERIALS	PROPERTIES
1.	Glazov & Vertman	1958	InSb, GaSb, AlSb	χ
2.	Glazov & Petrov (in Russian)	1958	InSb, GaSb, AlSb	η
3.	Amirkhanov & Magomedov	1964	InSb	κ
4.	Glazov & Chizhevskaya	1963	Ge, Si, ZnS	χ
5.	Blum & Ryabtsova	1958	InSb, GaSb	σ
6.	Busch & Vogt (in German)	1954	InSb	σ
7.	Glazov & Chizhevskaya	1961	Ge, AlSb, GaSb, InSb	σ
8.	Glazov & Chizhevskaya	1962	GaAs, InAs	σ & n
9.	Regel et.al.	1971	Sb_2 Se_3	σ & R
10.	Mogilevskii et.al.	1971	Sb_2 Te_3-Sb_2 Se_3	σ & κ
11.	Mogilevskii et.al.	1972	Sb, Te, Bi & Pb alloys	thermodiffusion
12.	Mogilevskii et.al.	1972	Te_X Se_{1-X}	σ & κ
13.	Fedorov & Machuev	1971	TlS, Tl_2S	κ
14.	Fedorov & Machuev	1971	GaSe, InSe	κ
15.	Mavlonov	1972	InSe, Ga_2Se_3	σ & κ
16.	Kazandzhan et.al.	1972	Te-Tl alloys	σ & TEP
17.	Kazandzhan et.al.	1971	I & Se impurities in Tl_2Te	σ & TEP
18.	Hodgkinson	1970	In-S & Tl-S	σ & theory
19.	Krestovnikov et.al.	1967	most semiconductors	Δv at melting
20.	Mal'agov & Magomedov	1969	$CuSbSe_2$	σ, κ & TEP
21.	Fedorov & Stil'bans	1967	Bi, Te, Sb, Se & Cu_2 Te	κ
22.	Fedorov et.al.	1968	Bi_2 Se_3	σ, κ & TEP

2.2 (Continued)

TABLE I (Continued)

REFERENCE	DATE	MATERIALS	PROPERTIES
23. Fedorov & Machuev	1967	Sb - Se alloys	κ
24. Fedorov & Machuev	1968	SbS	κ
25. Glazov et.al.	1967	AlSb, GaSb, InSb, InAs, GaAs	Tm, H_f, S_f
26. Perron	1970	Te_{1-x} Se_x	σ, κ
27. Cutler & Mallon	1964	Tl_x Te_{1-x}	σ & TEP
28. Enderby & Walsh	1966	CdSb, ZnSb, Bi_2Te_3, Sb_2Te_3	R, TEP & σ
29. Enderby & Simmons	1969	Au_2Te, CuTe, AgTe, Bi-Te, Tl-Te	R, σ
30. Cutler & Mallon	1966	Tl-Te solutions	σ, Seebeck coef.
31. Edmond	19[illegible]	As_2Se_3 - As_2Te_3 & As_2Se_3 - Tl_2Te_3	σ, TEP, optical absorption
32. Ioffe & Regel	1960	NaCl, [illegible], TlS_2, Bi_2O_3, Sb_2S_3, V_2O_5, Cu_2S-FeS, Si, Ge, GaSb, InSb, HgTe, HgSe, CdTe, Se, [illegible], TeSe, Bi_2Te_3, CuTe, [illegible]Se, ZnSb	σ, ρ, R, n TEP, mobility, κ
33. Regel, et.al	1970	Tl-Se, Tl-Te, Tl_2Te, Tl_2Se, Tl_2S, Sb_2Se_3, $CuSbSe_2$	σ, R, TEP
34. Regel, Smirnov, Shadrichev	1972	Sb_2Se_3, Ge, Si, InSb, GaSb, ZnSb, Bi_2Te_3, GeTe, SnTe, Te, Cu_2SnTe_3, PbTe, Cu_2GeTe_3, GaTe, Tl_xTe_y, $CuTlTe_z$	σ, κ, L/L_o
35. [illegible]son & Readall	1962	Cu_2S	κ

2.2 (Continued)

TABLE I (Continued)

REFERENCE	DATE	MATERIALS	PROPERTIES
36. Johnson & Readall	1963	$Cu_2S_{.25}Te_{.75}$, Cu_2S	κ
37. Cutler & Mallon	1962	Te, Te-Se alloys	κ, σ, TEP
38. Cutler & Mallon	1965	Tl-Te alloys	TEP, ρ_e
39. Lichter & Sommelet	1969	InSb, GaSb, AlSb, InAs, GaAs	$H_T^\circ - H_{298}^\circ$, c_p, $S_T^\circ - S_{298}^\circ$, $\frac{G_T^\circ - H^\circ_{298}}{T}$, T_m, ΔH_m, ΔS_m, S_T

TABLE II
LIQUID STATE PHYSICAL PROPERTIES REFERENCE LIST (BOOKS)

AUTHOR	TITLE	PROPERTIES	MATERIALS
McBride, Heimel, Ehlers, Gordon	Thermodynamic Properties to 6000°K for 210 Substances Involving the First 18 Elements, NASA SP-3001 (1963)	heat capacity, enthalpy, entropy, free energy	Al, Al_2O_3, B, B_2O_3, Be, BeO Li, LiCl, LiF, Li_2O, LiOH, Mg, MgF_2, Na, P, S, and Si
Mantell, Ed.	Engineering Materials Handbook (1958)	T_m, B.P., heat of fusion, density, vapor pressure, heat capacity, η, κ, σ, surface tension	Al, Sb, Bi, Cd, Cs, Ga, Au, In, Pb, Li, Mg, Hg, K, Rb, Ag, Na, Tl, Sn, Zn
Jackson, Ed.	Liquid Metals Handbook (1955)	isothermal compressibility, density, η, κ, σ, heat capacity, thermal diffusivity, Prandtl number	Na
Burdi	SNAP Technology Handbook, NAA-SR-8617 (1964)	T_m, B.P., density, η, κ, σ, heat capacity, surface tension, vapor pressure	Hg, Na, NaK, K, Rb, Li
Sharp	Thermodynamic Functions for Water -----, UCRL 7118 (1963)	P, V, T, entropy, enthalpy, internal energy, Gibbs free energy	H_2O

TABLE II (Continued)

AUTHOR	TITLE	PROPERTIES	MATERIALS
Svehla	Estimated Viscosities and Thermal Conductivities of Gases at High Temperatures, NASA TR-R-132 (1962)	Lennard-Jones constants, n, heat capacity	Al, AlCl, AlO, AlS, BF_3, BO, H_2O, Hg, $HgBr_2$, $HgCl_2$, HgI_2, Li, LiBr, LiO, Li_2, Li_2O, Mg, MgCl, MgF, Na, NaBr, NaCl, NaF, NaI, NaO, NaOH, O_2, P, Si, SiCl, SiF, SiO, SiS, Si_2, Xe, Zn
Madelung	Physics of III-V Compounds	atomic radii, T_m	B, C, N, Al, Si, P, Ga, Ge, As, In, Sn, Sb, Tl, Pb, Bi
Glazov, Glagoleva, Chizhevskaya	Liquid Semiconductors (1969)	electrical conductivity, σ thermoelectric power, T.E.P. density, ρ kinematic viscosity, ν magnetic susceptibility, χ melting temperature, T_M heat of fusion, Q_f mobility, ν	Si, Ge, Te, AlSb, GaSb, InSb, GaAs, InAs, ZnTe, CdTe, Ga_2Te_3, In_2Te_3, Mg_2Si, Mg_2Ge, Mg_2Sn, Mg_2Pb, GeTe, SnTe, PbTe, PbSe, PbS, Bi_2Se_3, Bi_2Te_3, Sb_2Te_3
Hultgren, Orr, Anderson and Kelley	Selected Values of Thermodynamic Properties of Metals and Alloys (1963)	heat capacity, c_p enthalpy, H_T-H_{st} entropy, S_T-S_{st} free energy, $\frac{F_T-H_{st}}{T}$ atomic weight, A_w vapor pressure, p	66 metals and semi-metals 167 alloys

TABLE II (Continued)

AUTHOR	TITLE	PROPERTIES	MATERIALS
Gray, Ed.	AIP Handbook (1963)	isothermal compressibility, β surface tension, σ thermal expansion coefficient, α thermal conductivity, κ	H_2O,Hg,Al,Sb,Bi,Cd,Cu,Ge, Au,Pb,Hg,Pt,K,Ag,Na,S_n,Zn H_2O,Hg,Li,Na,Pb,Sb,Sn,Te,Zn
Davydov	Germanium (1966)	heat capacity, C_p melting temperature, entropy, enthalpy: T_m,S_m,H_m Lennard-Jones parameters, ε&b_o molecular volume, v_o	Ge
Beer, Ed.	Liquid Metals - Chemistry and Physics	thermal coefficient of resistivity, isothermal compressibility, thermal expansion coefficient, η, heat capacity, surface tension, Hall coefficient, resistivity, magnetic susceptibility	All metals and semi-metals, many alloys

2.2 (Continued)

where L is a characteristic length for the liquid system. To obtain values of η_m in poise, the usual viscosity unit, the following conversions are used:

$$1 \text{ gauss} = 10^{-1} \frac{\text{dyne sec}}{\text{coul cm}} \qquad \text{and}$$

$$1 \text{ poise} = 1 \frac{\text{dyne sec}}{\text{cm}^2}$$

The meaning of the magnetic viscosity is indicated by a dimensionless parameter, the Hartmann number, which is defined as

$$h = \sqrt{\eta_m/\eta} \tag{2}$$

where η is the molecular viscosity of the melt. Thus if $h > 1$, then the magnetic viscosity predominates, while for $h < 1$, magnetoviscosity is not as important. Figures 1, 2 and 3 are graphs of Hartmann number versus magnetic induction for various materials, values of L and, in the case of sodium, different values of temperature. These graphs show that, while liquid sodium is, as expected, most affected by a magnetic field, the III - V compounds InSb, InAs and GaAs do show a definite field-induced viscosity with $h > 1$ for fields > 40 gauss and $L > 1$ cm. A field of 40 gauss is quite modest. Thus magnetic viscosity dominates for most of the conditions shown in the figures.

Convection Decay in a Magnetic Field

The Navier-Stokes equation describing bulk liquid motion in a magnetic field may be written

$$\rho \frac{d\vec{u}}{dt} = \vec{\Sigma} + (\vec{J} \times \vec{B}) \tag{3}$$

where $\vec{\Sigma} = -\vec{\nabla} [\rho\psi + P - \frac{\eta}{3} \vec{\nabla}\cdot\vec{u}] + \eta \nabla^2\vec{u}$ contains all non-electromagnetic forces. From the expression for the current density, $\vec{J}$, in a moving medium and from appropriate vector identities, it can be shown that

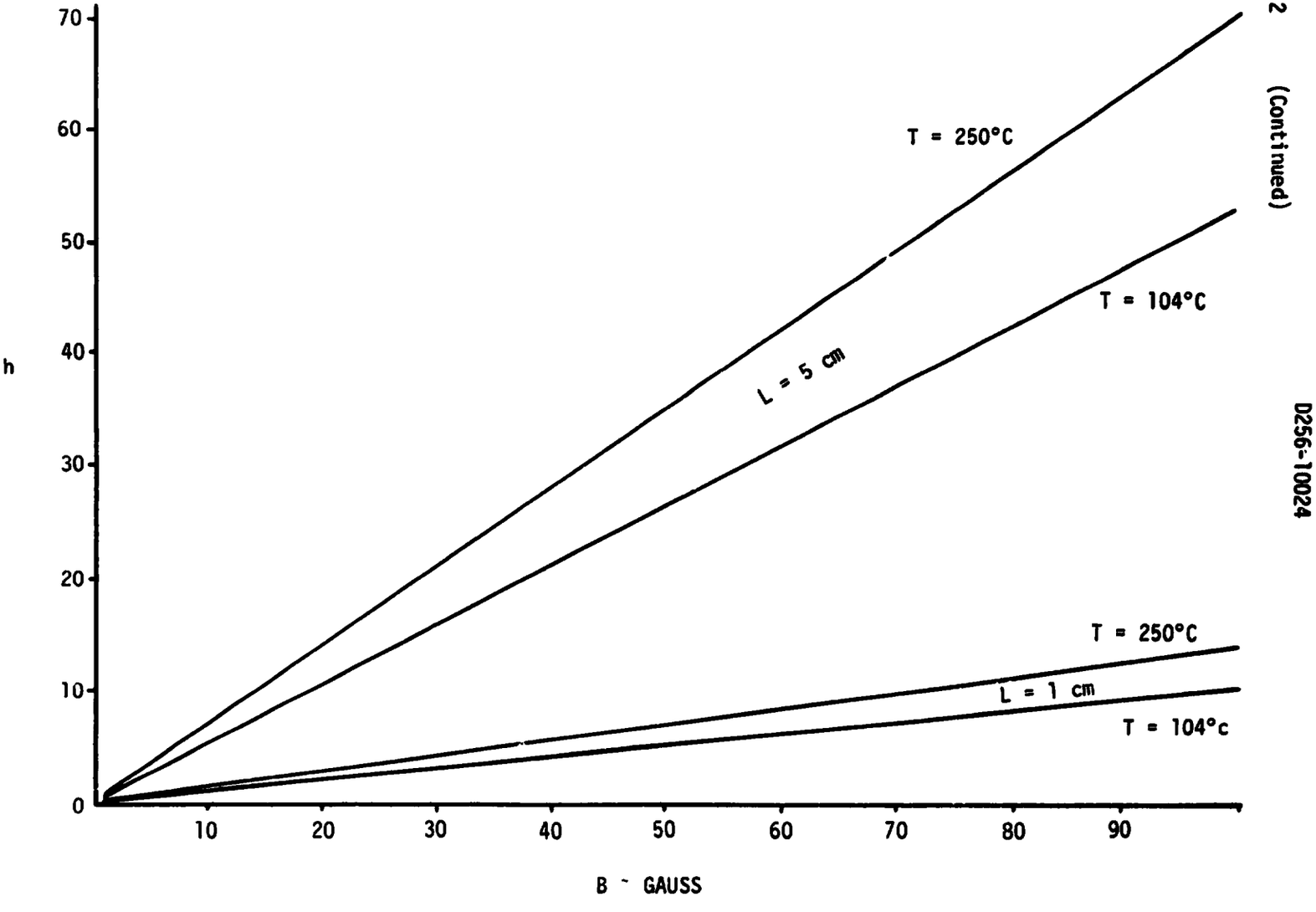

FIGURE 1: HARTMANN NUMBER VS. MAGNETIC INDUCTION
LIQUID SODIUM

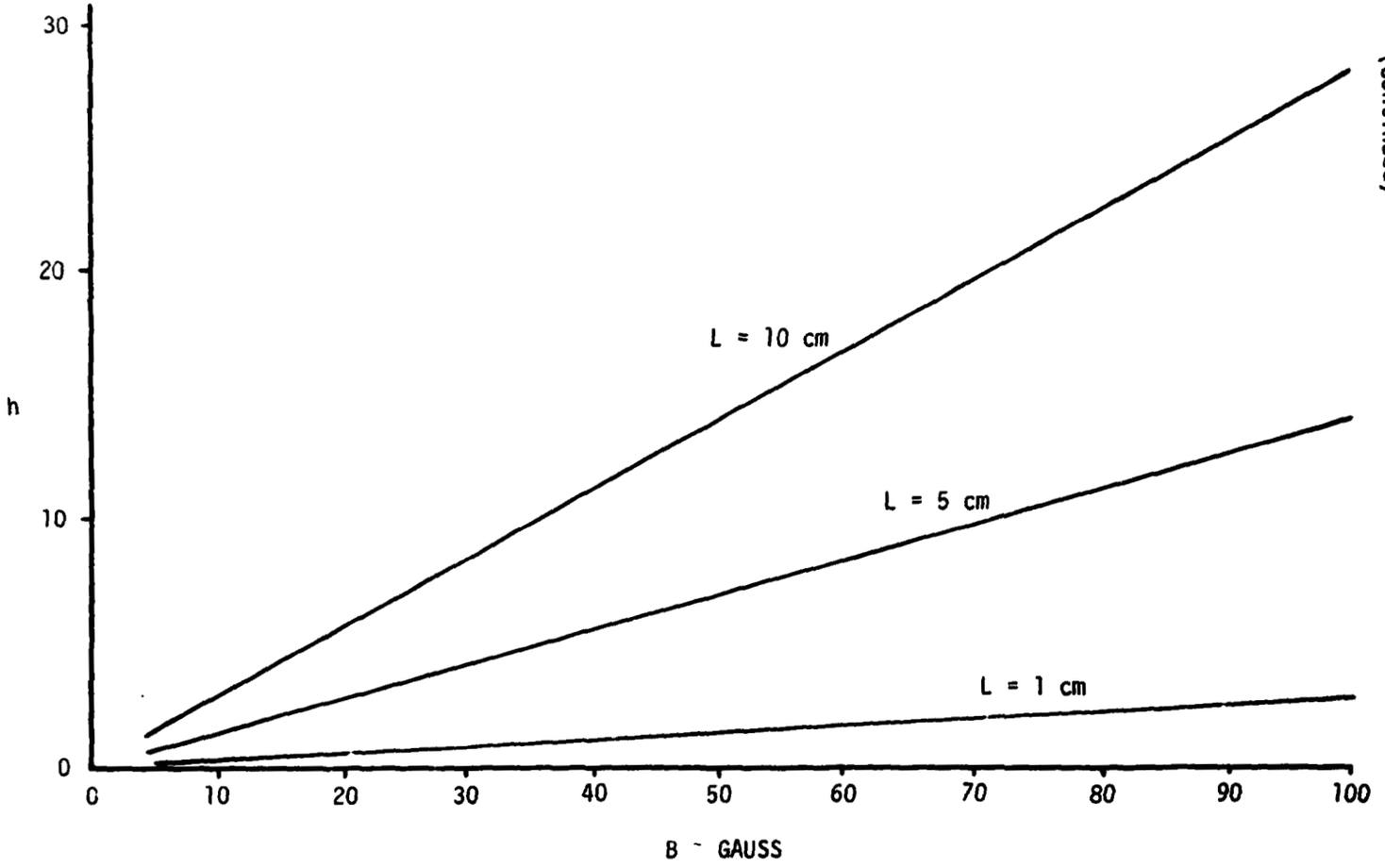

FIGURE 2: HARTMANN NUMBER VS. MAGNETIC INDUCTION
LIQUID InSb

2.2 (Continued)

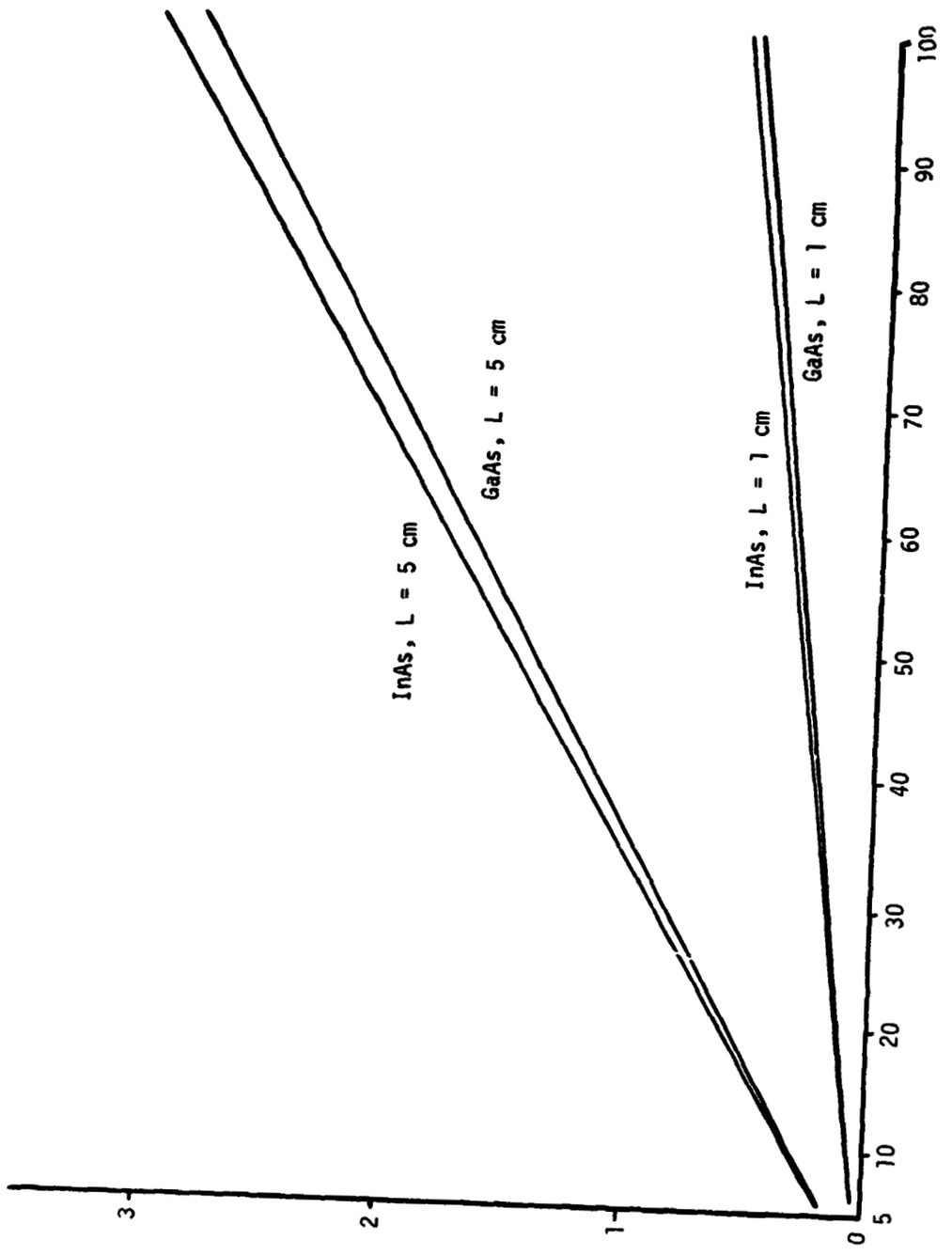

FIGURE 3: HARTMANN NUMBER VS. MAGNETIC INDUCTION
LIQUID InAs
LIQUID GaAs

2.2 (Continued)

the component of magnetic force transverse to the magnetic field lines is

$$(\vec{J} \times \vec{B})_t = -\sigma B^2 \vec{u}_t \quad . \tag{4}$$

If one considers only transverse components of equation (3) and defines a time constant, τ, by

$$\tau = \frac{\rho}{\sigma B^2} \tag{5}$$

equation (3) may be rewritten as

$$\frac{d\vec{u}_t}{dt} + \frac{1}{\tau} \vec{u}_t = \frac{\vec{\Sigma}_t}{\rho} \tag{6}$$

If it is assumed that the forces contained in $\vec{\Sigma}_t$ change only slowly with time, (6) may be integrated to yield

$$\vec{u}_t = \frac{\tau}{\rho} \vec{\Sigma}_t + (\vec{c}_o - \frac{\tau}{\rho} \vec{\Sigma}_t) e^{-t/\tau} \tag{7}$$

where $\vec{c}_o$ is an integration constant equal to the free convection velocity at time = t_0, the magnitude of which is on the order of 30 to 40 cm/sec. Figure 4 presents the qualitative decay curve for a situation corresponding to equation (7). Thus when a magnetic field is imposed on a melt in which convection currents are flowing, the flow velocity will be damped by the field according to equation (7), falling off after times much greater than τ to a value

$$\vec{u}_t \ (t >> \tau) \approx \frac{\tau}{\rho} \vec{\Sigma}_t \quad .$$

From equation (3), if there were no magnetic field,

$$\vec{\Sigma}_t \approx \frac{\rho}{t} \vec{c}_o \ , \quad \text{so}$$

$$\vec{u}_t \ (t >> \tau) \approx \frac{\tau}{t} \vec{c}_o << \vec{c}_o$$

2.2 (Continued)

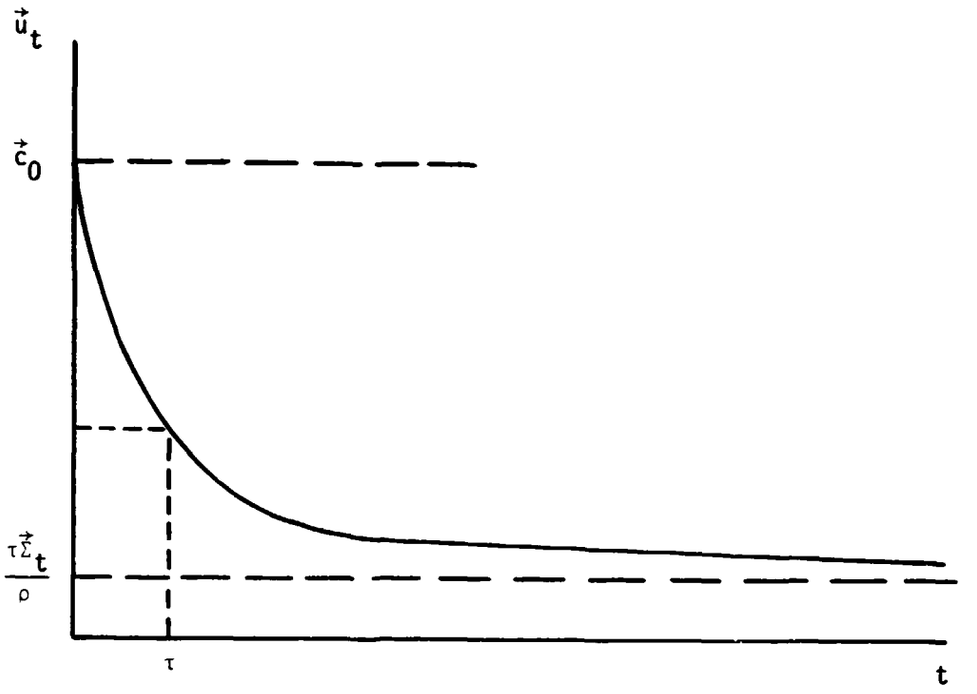

FIGURE 4: CONVECTION DECAY IN A MAGNETIC FIELD

For liquids of density $\rho = 6 \frac{gm}{cm^3}$, conductivity of $\sigma = 10^3\ \Omega^{-1}\ cm^{-1}$ and a magnetic induction of 10^3 gauss, τ is on the order of 6 seconds. Assuming that $\vec{c}_0 \simeq 35 \frac{cm}{sec}$, the velocity after three minutes will fall to about one cm/sec.

Body Forces Due to Oscillating Magnetic Fields

The qualitative aspects of oscillating magnetic fields have been discussed in References 1 and 2. Since the body force in $\frac{dynes}{cm^3}$ on an element

2.2 (Continued)

of liquid is given by the cross product of the eddy current, $\vec{J}_e$, and the magnetic induction, $\vec{B}$, the magnitude of this "eddy current force" is

$$f_e = |\vec{J}|\ |\vec{B}| \sin\theta \tag{8}$$

where θ is the angle between the $\vec{J}$ and $\vec{B}$ vectors. f_e then assumes its maximum value when $\theta = \frac{\pi}{2}$, which is often the case experimentally. By relating the eddy current to the field inducing it, one can show[3] that

$$f_{e_{max}} = |J|\ |B| = \frac{2}{a}HB = \frac{2\mu}{a}H^2 = \frac{2\mu_o}{a}(1+\chi)H^2 \tag{9}$$

where a is a characteristic length in the liquid, such as the radius of a cylindrical melt container. If one assumes that a is 5 cm, then

$$\frac{2\mu_o}{a} = 0.05028\ \frac{\text{dyne}}{\text{cm amp}^2}$$

Thus, the eddy current body force of equation (9) may be plotted as a function of field for different materials (different susceptibilities, χ) as in Figure 5. In practice, since values of χ for liquid metals and semiconductors are on the order of 10^{-6} cgs units, curves for the materials InSb, Ge, Na and Hg all fall on the same points to within 0.001%.

To gain a more quantitative feeling for the magnitude of the eddy current body force, it is helpful to compare it to the magnetoviscous force arising from the magnetic viscosity discussed earlier and to the gravitational body force, ρg. From equation (4), the magneto-viscous force may be written

$$f_m = \sigma\, \mu_o^2\, (1+\chi)^2\, H^2\, u \tag{10}$$

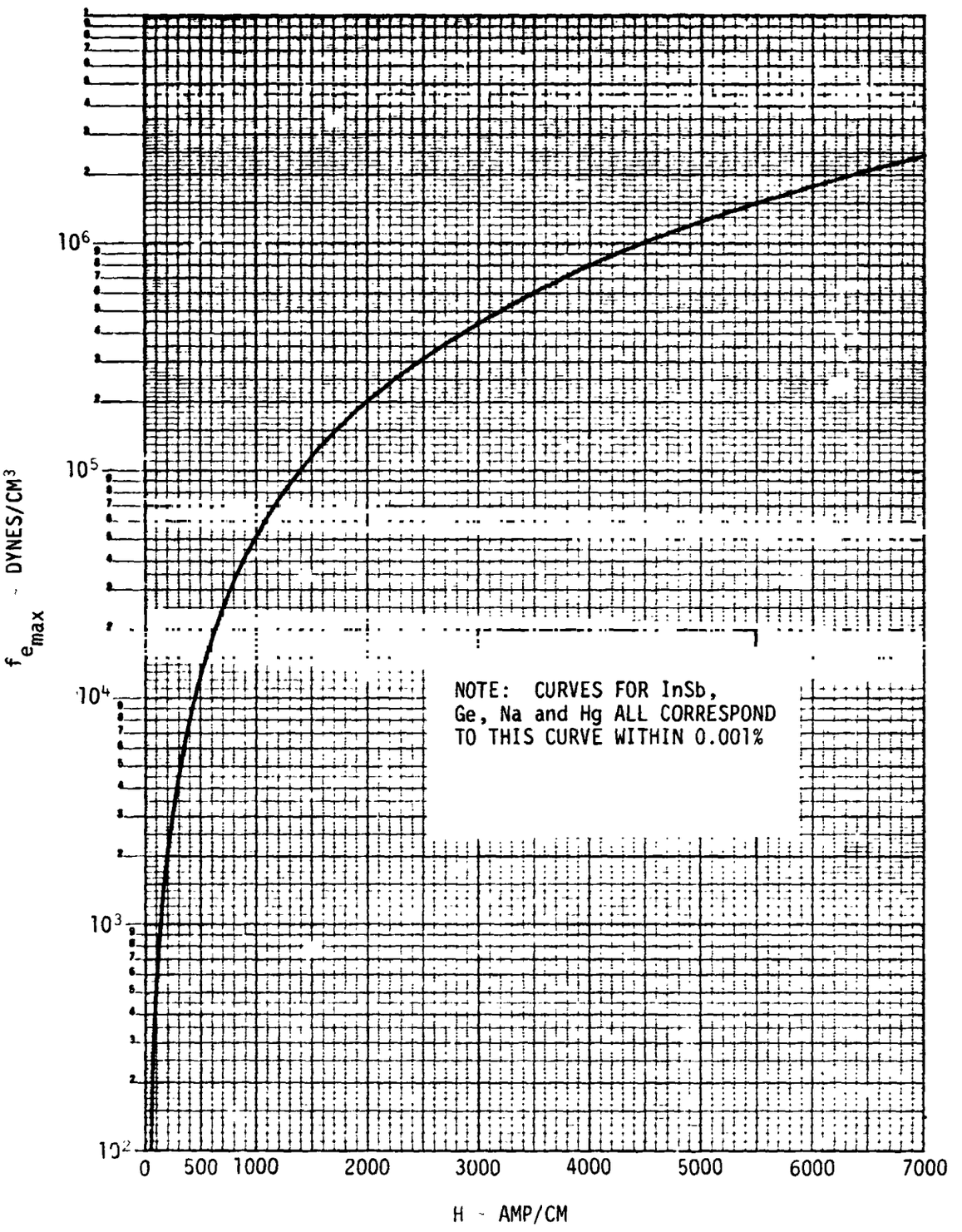

FIGURE 5: EDDY CURRENT BODY FORCES ON SEMICONDUCTOR MELTS

2.2 (Continued)

Thus by dividing equation (9) by (10) one obtains

$$\frac{f_{e_{max}}}{f_m} = \frac{2}{\sigma \mu_o a(1+\chi)u} \tag{11}$$

where it must be remembered that $f_{e_{max}}$ and f_m are vectorially in different directions, and in fact are often orthogonal. Assuming again that a = 5cm, $\sigma = 10^3\ \Omega^{-1}cm^{-1}$ and noting that $1+\chi \approx 1$ and $\mu_o = 4\pi \times 10^{-9}\ \Omega$ sec/cm, one may plot the ratio $f_{e_{max}}/f_m$ for a range of convection velocity values as in Figure 6. This graph shows that the predominance of the eddy current force increases for a diminishing or damped convective flow. Thus in using oscillating magnetic fields to control convection, or even to achieve stirring of the melt, one must be careful not to "overdamp" or set up eddy current-driven flows which are more vigorous than the gravity-driven convection at the beginning of the process.

To determine just how the eddy current force compares to the force driving natural convection, equation (9) is divided by the gravitational body force

$$f_{e_{max}}/f_g = \frac{2\mu_o (1+\chi)}{a\, g} \frac{H^2}{\rho} \tag{12}$$

For a = 5cm, $1+\chi \approx 1$, $\mu_o = 4\pi \times 10^{-2} \frac{dyne}{amp^2}$ and $g = 980 \frac{cm}{sec^2}$, this equation becomes

$$f_{e_{max}}/f_g = (5.13 \times 10^{-5} \frac{dyne\ sec^2}{amp^2\ cm^2}) \frac{H^2}{\rho} \tag{13}$$

which is plotted in Figure 7. It is obvious that $f_{e_{max}}$ dominates the liquid flow for field strengths above $500 \frac{amp}{cm}$. Liquid sodium is the most responsive, of the materials considered, to the eddy current force, while the semiconductors InSb and Ge fall between sodium and mercury in their response to the field. Thus it is seen that oscillating magnetic

2.2 (Continued)

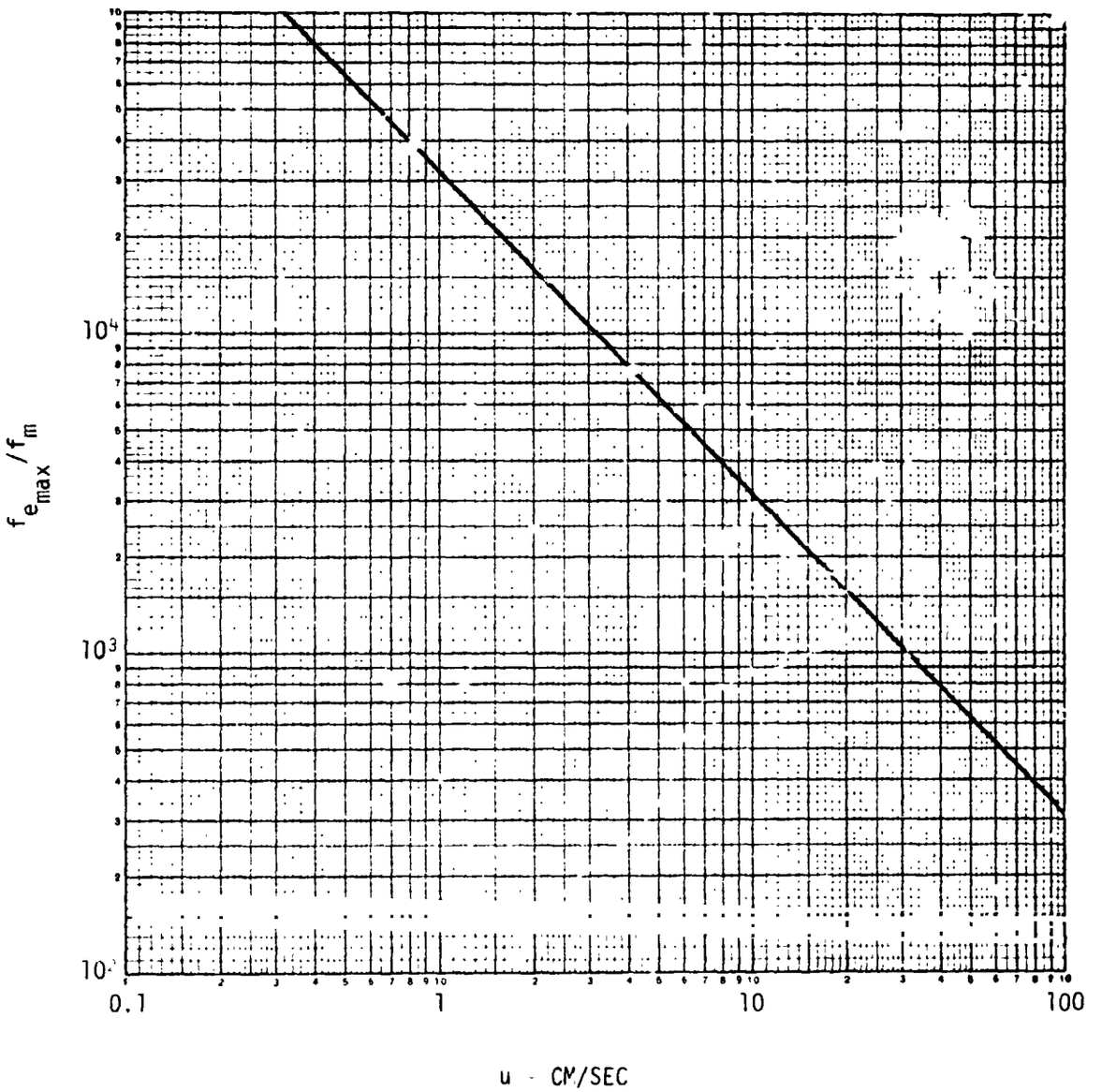

FIGURE 6: EDDY CURRENT/MAGNETOVISCOUS FORCE COMPARISON

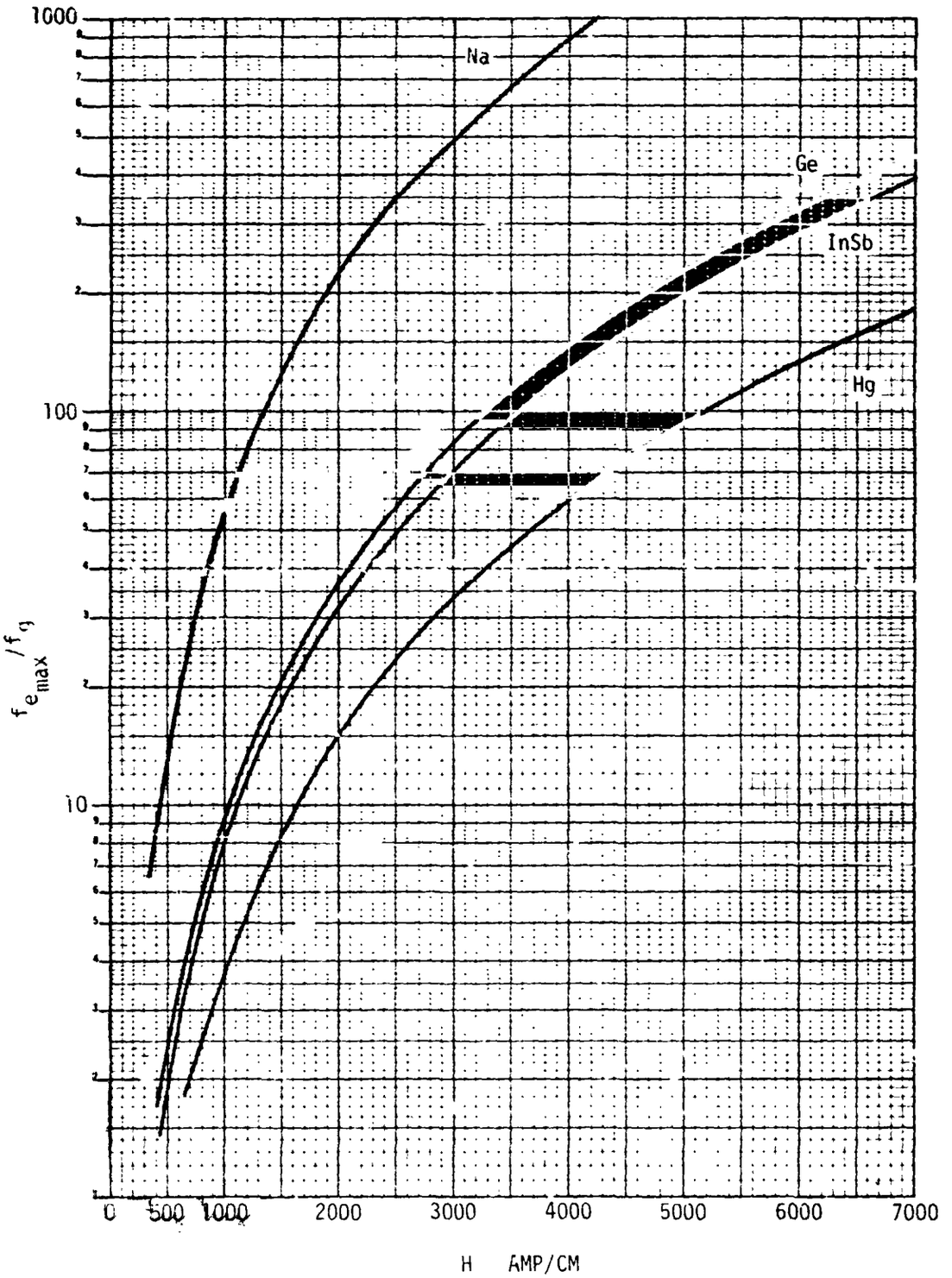

FIGURE 7: EDDY CURRENT/GRAVITY BODY FORCE COMPARISON

2.2 (Continued)

fields of even modest strengths (500 - 10,000 $\frac{amp}{cm}$) produce forces which are quite powerful compared to other forces in melts.

2.3 EXTERNAL FIELD EFFECTS DERIVED FROM THE FREE VOLUME MODEL

The effects which magnetic and gravitational fields have on the temperature, volume, Gibbs free energy, diffusion coefficient and solidification rate of solidifying melts have been described qualitatively in Reference 1. That analysis may be carried further by considering the ratio of the solidification rate under changed field conditions, U_c', to the solidification rate under normal field conditions, U_c. "Normal" field conditions implies zero magnetic field and 980 $\frac{cm}{sec^2}$ gravity, while "changed" field conditions means either an applied magnetic field or microgravity conditions existing in an orbital laboratory or other zero gravity simulator. Using Turnbull's expression[4] for the solidification rate (see equation 28 in Reference 1), and assuming that the fraction of lattice sites in a liquid-solid interface to which molecules can be attached remains constant, the field effect on solidification rate may be expressed as

$$\frac{U_c'}{U_c} = \frac{D'}{D} \frac{1 - e^{\Delta G'/kT'}}{1 - e^{\Delta G/kT}} \tag{14}$$

The Free Volume Model expression for the diffusion coefficient, D, may be written[5]

$$D = \frac{\psi}{3} \bar{u} v^* e^{-\frac{\gamma v^*}{v_f}} \tag{15}$$

where ψ is a parameter relating the distance traveled by a molecule between collisions to the average specific volume, v, of the liquid, and γ is an overlap factor lying between $\frac{1}{2}$ and 1. v^* is the critical value of free volume for the onset of diffusion, $\bar{u}$ is the gas kinetic velocity given by

$$\bar{u} = \sqrt{\frac{3kT}{m}} \tag{16}$$

2.3 (Continued)

and v_f is the free volume defined as

$$v_f = v - v_o \tag{17}$$

where v_o is the molecular volume calculated from the diameter and m is the molecular mass.

Now if equations (16) and (17) are substituted into (15), one obtains

$$D = \phi T^{\frac{1}{2}} e^{-\frac{\gamma v^*}{v}} (1 - v_o/v)^{-1} \tag{18}$$

where $\phi = v^* (\frac{\psi^2 k}{3m})^{\frac{1}{2}}$ is a constant for a given material and values of $\frac{\gamma v^*}{v}$ have been tabulated by Cohen and Turnbull[6] for some simple liquids.

Since T and v are the only variables in equation (18), the temperature and specific volume under altered field conditions may be expressed as

$$T' = T + \Delta T \quad \text{and} \quad v' = v + \Delta v$$

where ΔT and Δv are the temperature and specific volume changes produced by field changes. Writing the expression for D' in terms of T' and v' then dividing by equation (18) yields the relation for the field effect on diffusion coefficient

$$\frac{D'}{D} = (1 + \frac{\Delta T}{T})^{\frac{1}{2}} e^{f(v,\Delta v)} \tag{19}$$

where

$$f(v,\Delta v) = (\frac{\gamma v^*}{v}) (\frac{\Delta v}{v}) [(1 - \frac{v_o}{v})^2 + \frac{\Delta v}{v} (1 - \frac{v_o}{v})]^{-1}$$

Thus to determine the effects of magnetic fields or microgravity on U_c and D, the terms $\frac{\Delta T}{T}$, $\frac{\Delta v}{v}$ and the altered free energy, $\Delta G'$, need to be calculated.

Temperature, Volume and Free Energy Changes in Microgravity

From the definition of isothermal compressibility[7] the fractional

2.3 (Continued)

change in the volume of a liquid due to a change in pressure, ΔP is

$$\frac{\Delta v}{v} = -\beta \Delta P \tag{20}$$

where β is the isothermal compressibility of the liquid. If a container of liquid is envisioned as being moved from the Earth's surface into an orbiting laboratory where microgravity conditions prevail, there will be a change in the hydrostatic pressure within the liquid of

$$\Delta P = -\rho z \Delta g \tag{21}$$

where ρ is the liquid density, z is depth below the liquid free surface on Earth and Δg is the change in gravity or acceleration field. Thus from Equation (20)

$$\frac{\Delta v}{v} = \beta \rho z \Delta g \tag{22}$$

From the definition of the thermal expansion coefficient, α, one can write[7]

$$\frac{\Delta T}{T} = \frac{\Delta v / v}{\alpha T} \tag{23}$$

so the temperature change corresponding to the pressure-induced volume change may be calculated from (22).

Since the Gibbs free energy of solidification is given[8] by

$$\Delta G = S_c \delta T \tag{24}$$

where S_c is the entropy of solidification and δT is the amount of undercooling (a negative number), external effects must be of the form

$$\Delta G' = \Delta G + \Delta v \Delta P \tag{25}$$

or from (20)

$$\Delta G' = \Delta G - \beta v (\Delta P)^2 \tag{26}$$

2.3 (Continued)

with ΔP given by equation (21) for a microgravity case. With these equations, the free energy term

$$(1 - e^{\Delta G'/kT'}) / (1 - e^{\Delta G/kT}) ,$$

the diffusion coefficient change D'/D, and the solidification rate change U_c'/U_c may be calculated for any material if the characteristic parameters are available for the liquid state of the subject material. Table III lists values of the parameters required for calculations in both the microgravity case and in the magnetic field case for four representative materials.

Temperature, Volume and Free Energy Changes in a Magnetic Field

Equation (20) may be used to determine fractional volume changes in a liquid placed in a magnetic field if ΔP is now the magnetic pressure[9]

$$\Delta P = - \frac{1}{2} \mu_o [H_o^2 - \chi H^2] \qquad (27)$$

where μ_o is the permeability of free space (.1257 dyne/amp^2), χ is the magnetic susceptibility, H_o is the initial field strength before the liquid was placed in the field and H is the resulting steady-state of the field internal to the liquid. Thus

$$\frac{\Delta v}{v} = \frac{1}{2} \beta \mu_o [H_o^2 - \chi H^2] \quad . \qquad (28)$$

To estimate $\Delta v/v$ without having to specify boundary conditions of a particular system, one may assume that for paramagnetic or diamagnetic liquids, $H \simeq H_o$. Since χ is on the order of 10^{-7} for such liquids,

$$\frac{\Delta v}{v} \simeq \frac{1}{2} \beta \mu_o (1-\chi) H^2 \simeq \frac{1}{2} \beta \mu_o H^2 \quad . \qquad (29)$$

An alternative method for calculating the volume change would be to use the theory of magnetostriction[10]. Unfortunately several parameters required in the equations of this theory are not available for liquids.

TABLE III PARAMETERS USED FOR CALCULATING FIELD EFFECTS*

MATERIAL	χ_ℓ cm^{-3}	χ_s cm^{-3}	Q erg/cm^3	β $cm^2/dyne$	α $^\circ K^{-1}$	S_c $erg/mole^\circ K$	$\frac{\gamma v^*}{v}$	v_o $cm^3/mole$	v $cm^3/mole$	T $^\circ K$	ρ_ℓ gm/cm^3
InSb Reference	-6.816×10^{-7} 13	-7.612×10^{-7} 13	2.69×10^{6} 11&14	3.15×10^{-11} 20	.000341 20	6.211×10^{8} 14	0.1 E	10.8 E	18.2 39	793	6.43 39
Ge Reference	-4.902×10^{-7} 13	-6.125×10^{-7} 13	2.15×10^{6} 11&14	1.19×10^{-11} 20	.0001574 20	2.443×10^{8} 15	0.3 E	6.8 E	13.0 39	1200	5.57 39
Hg Reference	-2.466×10^{-6} 18	-2.128×10^{-6} 18	1.52×10^{5} 11&14	3.9×10^{-12} 16	.00018 16	9.8×10^{7} 14	.0935 6	8.5 E	14.6 17	224	13.7 17
Na Reference	5.859×10^{-7} 19	4.896×10^{-7} 18	1.02×10^{5} 11&14	1.916×10^{-11} 17	.00028 18	7.01×10^{7} 14	.236 6	17.3 E	24.6 17	361	0.93 17

* H is assumed to be 10^5 oersteds (7.96×10^4 amp/cm)

δT is assumed to be $-10^\circ K$ ($T = T_m + \delta T$)

Z is assumed to be 1 cm

E indicates estimated values

2.3 (Continued)

In his paper describing magnetic field effects on the dissolution and solidification rates of paramagnetic crystals in solution, Schieber[11] derived the following expression for the change in temperature of a solidifying system due to the application of a magnetic field, H

$$\frac{\Delta T}{T} = (\chi_\ell - \chi_s)\frac{H^2}{4Q} \tag{30}$$

where χ_ℓ is the magnetic susceptibility per unit volume of the liquid, χ_s is the susceptibility of the solid and Q is the latent heat of solidification. Thus the temperature at the interface of a solidifying material in a magnetic field can increase or decrease depending on whether the material is diamagnetic or paramagnetic and on the relative magnitudes of χ_ℓ and χ_s.

The Gibbs free energy of a material in a magnetic field is given by Wood[12] as

$$G' = G - v\vec{H}\cdot\vec{M} \tag{31}$$

where M is the magnetization, χH. Thus the change in G at the interface with a magnetic field applied will be

$$\Delta G' = \Delta G - v(\chi_\ell - \chi_s)H^2 \quad . \tag{32}$$

It is easy to show that if $S_c\delta T > 4vQ$, the free energy term

$$(1 - e^{\Delta G'/kT'}) \;/\; (1 - e^{\Delta G/kT})$$

is less than unity if $\chi_\ell - \chi_s$ is positive and becomes greater than one if $\chi_\ell - \chi_s$ is negative.

Calculation of Field Effects on Melts

From equations (22),(23),(26),(29),(30) and (32) and the parameter values given in Table III, the various terms in equations (14) and (19) can be calculated and used to determine values for D'/D and U_c'/U_c for both the microgravity

2.3 (Continued)

and magnetic field cases of altered external field conditions. Note that the references for the input data are indicated under the appropriate values in Table III. Values of the variable parameters which were assumed for the examples presented here are given below the table, and estimated values of v_0 and $\frac{\gamma v^*}{v}$ were determined from atomic and ionic radii shown on the Sargent-Welch Table of Periodic Properties of the Elements (1968). In such estimations a 50% composition for InSb is assumed.

The values for U_c'/U_c, D'/D and the free energy term which were computed from equations (14) and (19) are given in Table IV. Several comments should be made concerning the Free Volume Model and the results presented in Table IV. First, Turnbull's model is based on such simplifying assumptions that it could be expected to be most accurate for the simplest liquids. But when the model is compared with experimental data (see Table I, Reference 20), it is found to be more accurate for water and methanol than for such simple liquids as Argon and Helium. In addition, Turnbull's purpose in developing the model was to describe transport and solidification in glass-forming liquids, but he also gets good agreement with experiment for organic liquids as well as liquid metals[6]. So there is little or no correspondence of the model to particular classes of liquids. On the other hand, because of the simplifying assumptions, the model is not overly accurate for any specific liquid[20]. But it can provide order-of-magnitude estimates for quantities of interest, and at least indicate the direction of change in these quantities under the influence of perturbing fields. This is the primary benefit of the model to Space Processing - that it does allow the determination of direct effects of magnetic and gravitational fields on diffusion coefficients and solidification rates. By "direct effect" is meant those effects derivable directly from the fields themselves, and not related to convective or magnetohydrodynamic effects. Such effects, shown in Table IV, can be expressed as percent changes if one notes that for numbers as close to unity as these, the percent change in

TABLE IV

EXTERNAL FIELD EFFECTS ON REPRESENTATIVE MATERIALS

MATERIAL	MICROGRAVITY CASE			MAGNETIC FIELD CASE		
	FREE ENERGY TERM	D'/D	U_c'/U_c	FREE ENERGY TERM	D'/D	U_c'/U_c
InSb	0.9999993	1.0000005	0.9999998	0.99993	1.00742	1.007
Ge	0.99999966	1.0000003	0.99999996	0.99987	1.00624	1.006
Hg	0.9999987	1.0000007	0.9999994	1.00539	0.99805	1.003
Na	0.99999983	1.0000001	0.99999993	0.99771	1.02139	1.019

2.3 (Continued)

a quantity X is approximately 100 (X'/X-1) where X' is the perturbed value. Expressed this way, the changes in both diffusion coefficients and solidification rate are in the ranges 10^{-5} to 10^{-6}% for the microgravity case and 0.3 to 1.9% for the magnetic field case.

It must be noted that the changes in D and U_c in the magnetic field case are strongly dependent on field strength. That is, for high enough fields, the value of D'/D for mercury could be greater than one, while for sufficiently low fields, the values of D'/D for InSb, Ge and Na could be less than one. But the data do show that gravity has a much smaller direct effect on D and U_c than do magnetic fields. Thus this analysis supports the thesis that suppression of gravity-driven convection, which has an indirect effect on solidification parameters, is the primary benefit of materials processing in space. The data in Table IV also show that the free energy term is less sensitive to magnetic field changes than is the diffusion coefficient. This is due to the more direct dependence of the diffusion coefficient on field-induced volume change and to the fact that volume changes are much larger (by factors proportional to H^2) in magnetic fields than in microgravity where $\frac{\Delta V}{V}$ is on the order of 10^{-8}. The increase in U_c upon the application of a magnetic field indicated in Table IV has been observed experimentally by Schieber[11].

2.4 THE RELATION OF EXTERNAL FIELDS TO SOLUTE DISTRIBUTION IN SOLIDS

Previous sections of this report have dealt with calculations performed with theories developed during the period described by Reference 1. The present contract was primarily concerned with such calculations, but also provided for further theoretical development in the area of external field effects on solute distribution in solids. The question addressed by this portion of the work could be stated: "Is it possible to develop a theoretical model which will describe the effects an

2.4 (Continued)

external field has on the substructure of a material which solidifies in the field?" The best answer to this question at present is that a model consisting of four steps has been developed which formally relates the occurrence of microsegregation in a solid to the external field conditions which might obtain during solidification of a binary material. The steps are:

1. Calculate the field distribution inside the melt due to the known external field as a function of susceptibility (magnetic field case) or density (gravitational field case).

2. Find the force the internal field exerts on solute atoms.

3. Determine the resulting solute atom velocity produced by the force.

4. Use Sekerka's interface stability theory to relate the criteria for microsegregation to solute atom velocity.

Although the model yields a formal relation between external fields and microsegregation, it is not really useful for performing practical calculations since each step contains operations which cannot be performed rigorously for most real solidification situations. However, it is instructive to consider the theoretical aspects of each of the above steps.

Field Distributions in Melts

The calculation of magnetic field distributions $\vec{H}(\vec{r},t)$, in materials from a known field outside the material has long been understood[21].

Basically, one solves Laplace's equation

$$\nabla^2 \phi = 0 \tag{33}$$

for the magnetic potential, ϕ, where

$$\vec{H} = - \vec{\nabla} \phi \tag{34}$$

2.4 (Continued)

in all regions of space subject to the boundary conditions of the problem. As in all field problems, the geometry of the situation determines the form of the boundary conditions and the solutions. Figure 8 shows the two geometries considered. These geometries were chosen because of their widespread experimental usage.

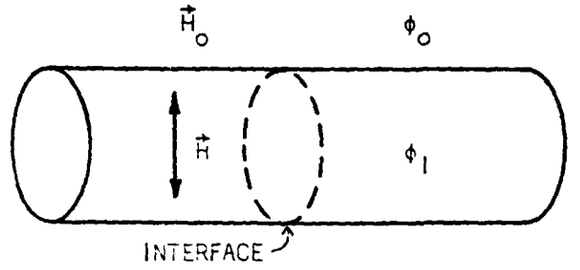

(A)

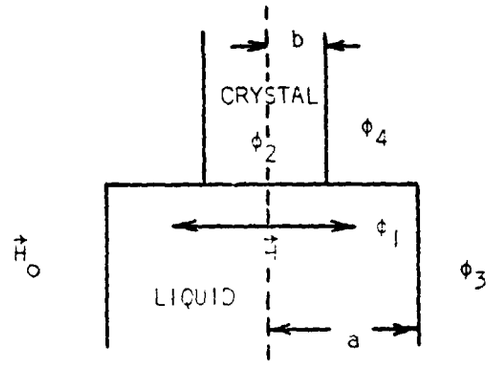

(B)

FIGURE 8: CRYSTAL-MELT GEOMETRIES CONSIDERED IN THE STUDY OF MAGNETIC FIELD DISTRIBUTIONS IN MELTS. (A) CORRESPONDS TO ZONE REFINING AND (B) TO CZOCHRALSKI CRYSTAL GROWTH.

2.4 (Continued)

The zone refining geometry can be considered an infinite cylinder, since the solutions of interest are those in a small region near the liquid-solid interface. The boundary conditions in this simple case are

$$\phi_1 (0,\theta) = \text{finite} \tag{35a}$$

$$\mu_1 \frac{\partial \phi_1}{\partial r}\Big|_a = \mu_0 \frac{\partial \phi_0}{\partial r}\Big|_a \tag{35b}$$

$$\phi_1 (a,\theta) = \phi_0 (a,\theta) \tag{35c}$$

$$\phi_0 (r,\theta) \underset{r \to \infty}{\longrightarrow} - H_0 r \cos\theta \tag{35d}$$

where ϕ_0 is the potential outside the cylindrical container, ϕ_1 is the potential inside and H_0 is the initial field before the melt was introduced into the field. The solutions obtained in the usual manner[21] are in cylindrical coordinates

$$\vec{H}_0' = H_0 [\cos\theta\, \hat{r} - \sin\theta\, \hat{\theta}] + \tag{36a}$$

$$\left(\frac{\chi}{2+\chi}\right) \frac{a^2}{r^2} H_0 [\cos\theta\, \hat{r} + \sin\theta\, \hat{\theta}]$$

$$\vec{H}_1 = \frac{2}{2+\chi} H_0 (\cos\theta\, \hat{r} - \sin\theta\, \hat{\theta}) \tag{37a}$$

and in rectangular coordinates

$$\vec{H}_0' = H_0 \hat{i} + \left(\frac{\chi}{2+\chi}\right) H_0 \frac{a^2}{r^4} [(x^2-y^2)\hat{i} + 2xy\,\hat{j}], \quad r^2 = x^2+y^2 \tag{36b}$$

$$\vec{H}_1 = \left(\frac{2}{2+\chi}\right) H_0 \hat{i} \tag{37b}$$

where $\hat{i}$, $\hat{j}$, $\hat{r}$ and $\hat{\theta}$ are unit vectors, with $\vec{H}_0 = H_0 \hat{i}$ initially.

The Czochralski geometry presents a much more difficult problem. First, because this case is essentially two cylinders of different radii

2.4 (Continued)

meeting end-to-end at the z=0 plane, there are more boundaries, and thus boundary conditions (see Appendix B) and solutions to be considered. Also, because the problem is not symmetrical on either side of the z=0 plane, the general solution to equation (33) is a Fourier-Bessel series

$$\phi = \sum_{km} [A_{km}J_m(kr) + B_{km}N_m(kr)] \quad X$$

$$[C_k e^{kz} + D_k e^{-kz}][E_m \cos m\theta + F_m \sin m\theta] \qquad (38)$$

and this series unfortunately does not converge in the region near the z=0 plane. Thus no rigorous analytical solution to this problem is possible, and one must choose either an approximate analytical solution or a numerical computer solution. An approach to obtaining an approximate solution is to convert the Czochralski geometry into the geometry of two infinite, concentric cylinders as shown in Figure 9. The solutions to the infinite concentric cylinder problem are easily obtained, then the solutions may be written above z=0 by setting $\mu_1 = \mu_0$ and below z=0 by setting $\mu_2 = \mu_1$.

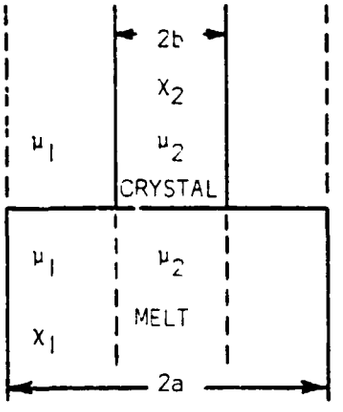

FIGURE 9: CONCENTRIC CYLINDER APPROXIMATION TO CZOCHRALSKI GEOMETRY.

2.4 (Continued)

Thus, in cylindrical coordinates

$$\vec{H}_0' = H_0 (\cos\theta\,\hat{r} - \sin\theta\,\hat{\theta}) + \frac{\chi}{2+\chi}\frac{d^2}{r^2} H_0 (\cos\theta\,\hat{r} + \sin\theta\,\hat{\theta}) \tag{39a}$$

where $\chi = \chi_1$ and $d = a$, $z < 0$; $\chi = \chi_2$ and $d = b$, $z > 0$

$$\vec{H}_1 = \frac{2}{2+\chi_1} H_0 (\cos\theta\,\hat{r} - \sin\theta\,\hat{\theta}) \tag{40a}$$

$$\vec{H}_2 = 2\left(\frac{1+\chi_2}{2+\chi_2}\right) H_0 (\cos\theta\,\hat{r} - \sin\theta\,\hat{\theta}) \tag{41a}$$

In rectangular coordinates, the solutions are

$$\vec{H}_0' = H_0\,\hat{i} + \frac{\chi}{2+\chi} H_0 \frac{d^2}{r^4}[(x^2-y^2)\hat{i} + 2xy\hat{j}] \tag{39b}$$

where $\chi = \chi_1$ and $d = a$ for $z < 0$; $\chi = \chi_2$ and $d = b$ for $z > 0$, $r^2 = x^2 + y^2$ and $\vec{H}_0'$ indicates the new field outside the melt,

$$\vec{H}_1 = \frac{2}{2+\chi_1} H_0\,\hat{i} \tag{40b}$$

$$\vec{H}_2 = 2\left(\frac{1+\chi_2}{2+\chi_2}\right) H_0\,\hat{i} \tag{41b}$$

The trouble with these solutions is, naturally, that they do not satisfy the real boundary conditions (see Appendix B) in the liquid-solid interface region, which is the region of primary interest. An approach to obtaining a solution which does satisfy the boundary conditions for the field distribution in a Czochralski growth system utilizing computer capabilities is the finite element method. This method consists basically of four steps:

1. Break up the region of interest (interface region) into small elements as shown in Figure 10.

2.4 (Continued)

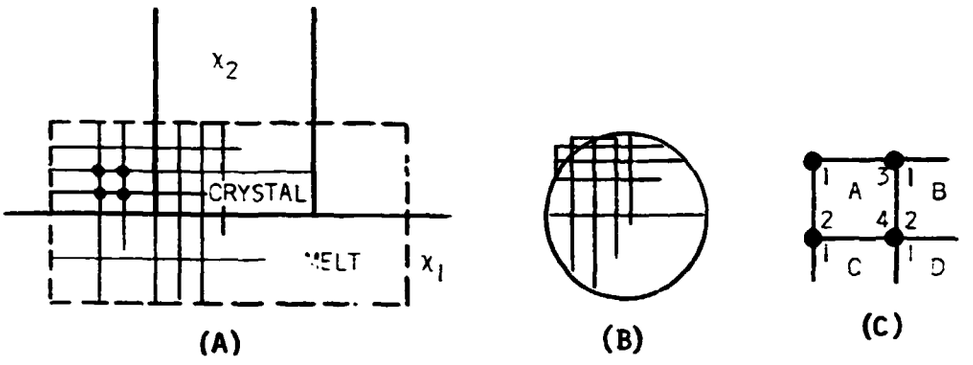

FIGURE 10: FINITE ELEMENT METHOD FOR SOLVING FIELD DISTRIBUTION PROBLEMS IN CZOCHRALSKI GEOMETRY

(A) ELEMENT GRID IN INTERFACE REGION - SIDE VIEW

(B) ELEMENT GRID IN INTERFACE REGION - VERTICAL VIEW

(C) NODES OF ADJACENT ELEMENTS

2. Solve Laplace's equation for ϕ at each node for each element.

3. Impose "compatibility" conditions on the nodes of element i so that solutions at each node of i satisfy the boundary conditions of each element adjoining i at that node, and therefore satisfy the boundary conditions of the problem.

4. Program the computer to sum the solutions for each element (which satisfy boundary or compatibility conditions) over all elements to obtain the total solution of the problem.

Techniques for actually carrying out the above steps are not yet perfected since the application of finite element methods to field theory problems is relatively new. Thus the time and resources required to obtain a solution for the field distribution in a Czochralski crystal

2.4 (Continued)

growth system are far beyond the scope of the present study. However, it is possible to determine qualitatively the shape of the field in the interface region. Physically, it is known that magnetic induction ($\vec{B}$) field lines are "pushed out" of materials possessing lower permeabilities than their surroundings. It can also be seen from equations (40) and (41) that $B_1 > B_2$. Therefore the lines of $\vec{B}$ in the interface will be shaped qualitatively as in Figure 11 when $\chi_1 > \chi_2$. Thus the qualitative field shape of Figure 11 coupled with the numerical answers from equations (39) - (41) constitute an approximate solution for the field distribution in the Czochralski growth case.

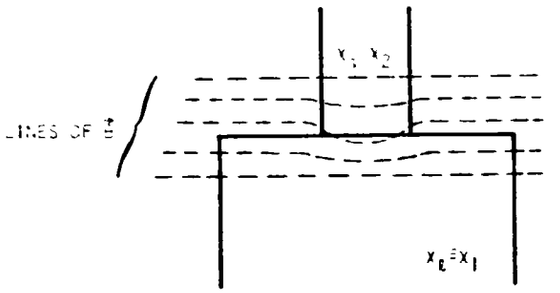

FIGURE 11: $\vec{B}$ FIELD LINES IN THE INTERFACE REGION, CZOCHRALSKI GEOMETRY, $\chi_1 > \chi_2$

Gravitational field distributions are even more difficult to calculate rigorously because they depend on the integrated matter distribution throughout the liquid-solid system as well as any external gravity field such as that of the Earth or the random acceleration field on a spacecraft. But order-of-magnitude estimates of gravitational forces on solute atoms may be found from $F = mg_T$ where m is solute atom mass and g_T is the total gravity field acting on it. On Earth g_T is the

2.4 (Continued)

sum of the Earth's mass field, its rotational acceleration field (these two sum to 1g) and the gravity field of the material in which the atom is situated.

For a melt in a cylindrical container, the gravity field due to the melt mass acting on a molecule near the surface of the melt may be estimated from Gauss's law[22]

$$\int\int \vec{g}_c \cdot d\vec{s} = -4\pi G \int\int\int \rho \, dv \tag{42}$$

where G is the universal gravitation constant and ρ is the density of the melt. Assuming ρ and $\vec{g}_c$ to be constant, equation (42) becomes

$$\vec{g}_c \cdot (z\hat{r}_c + r_c \hat{K}) = -2\pi G \rho r_c z$$

or

$$\vec{g}_c = -\pi G \rho \, (r_c \hat{r}_c + z\hat{K}) \tag{43}$$

where r_c is the radius of the cylinder, z is its length and $\hat{r}_c$ and $\hat{K}$ are the corresponding unit vectors. Now $\pi G\rho = 1.26 \times 10^{-6}$ sec^{-2}, so for values of r_c and z on the order of 10 cm, the magnitude of $\vec{g}_c$ is roughly 10^{-5} cm/sec^2 or 10^{-8} g. Therefore, if $\hat{r}_e$ represents a unit vector lying along a radius vector of the earth, the total gravity field in a cylindrically shaped melt is

$$\vec{g}_T = -g \hat{r}_e - 10^{-8} g \, (\hat{r}_c + \hat{K}) \simeq -g \hat{r}_e \quad . \tag{44}$$

In a space processing laboratory, the gravity level can be represented by

$$\vec{g}_T = -\vec{g}_c + \vec{f}\,(a) \tag{45}$$

where $\vec{f}(a)$ represents random spacecraft accelerations and vibrations which are on the order of 10^{-3}g to 10^{-6}g.

2.4 (Continued)

Resultant Internal Forces on Solute Atoms and Atom Velocity

Once the magnetic field distribution in a melt is known the force on a given atom due to the field is[21]

$$\vec{F}_{mag} = \vec{\nabla} (\vec{m}_i' \cdot \vec{B}) \tag{46}$$

where $\vec{m}_i'$ is the magnetic moment of the ith atom. Since $\vec{m}_i'$ is constant for a given species of atom, equation (46) can be written

$$\vec{F}_{mag} = (\vec{m}_i' \cdot \vec{\nabla}) \vec{B} \tag{47}$$

or, in terms of scalar differences

$$F_{mag} = m' \frac{\Delta B}{\Delta x} \tag{48}$$

The magnetic moment, m', may be calculated from the susceptibility of the material. Diamagnetic materials do not have magnetic moments as such, but do exhibit behavior in a magnetic field which corresponds to an "effective moment"[23]

$$m'_{dia} = -\frac{V}{N_o} H \tag{49}$$

where V is the volume per mole of diamagnetic liquid and N_o is Avogadro's number. For paramagnetic materials the moment is[24]

$$m'_{para} = \left[kT\left(\frac{3V_a}{N_o} + \frac{Zr_o^2}{2} - r^2\right)\right]^{\frac{1}{2}} \tag{50}$$

where the second term on the right derives from the diamagnetic contribution to the paramagnetic susceptibility. If any solute atom possesses a net electronic charge, it will also experience Lorentz forces as it moves in the magnetic field of the melt. This situation is considered in Appendix C.

Gravitational forces, as have been indicated, are calculated from

$$F_g = mg_T \tag{51}$$

2.4 (Continued)

where m is the mass of a solute atom. Interatomic forces are found from the negative gradient of the intermolecular potential, ϕ, for the solute-solvent system in question. A value for the force may be calculated if one assumes that 2-body forces predominate and assumes a particular form for the potential. For the Lennard-Jones potential[25]

$$F_{mol} = 24 \frac{\varepsilon}{r} \left[\left(\frac{\sigma}{r}\right)^{12} - \left(\frac{\sigma}{r}\right)^{6} \right] \qquad (52)$$

where ε and σ are the Lennard-Jones energy and distance parameters and r is the intermolecular separation. (The terms atom and molecule are used interchangeably since the simple models described here do not differentiate between molecules of different atomic structure.) Table V presents values of the forces calculated from equations 48 - 52 for several liquids.

One must be careful, when comparing these forces, to remember that they are not static. That is, if a liquid is envisioned as a collection of molecules situated in cells formed by their nearest neighbors, each molecule is known to oscillate about the center of its cell with a restoring force such as equation (52). But since diffusion is known to occur, at some instant the force and cell structure must be altered enough to allow the molecule to escape its original cell and enter another. This alternation of the cell structure and restoring force, or cell potential, will occur randomly because, as must be recalled, each molecule making up the cell under discussion is also oscillating in its cell. Of course, even this picture is an oversimplification because the description of liquid forces is one of the most difficult of the N-body problems. So although the data of Table V indicate that liquid intermolecular forces are much stronger than magnetic or gravitational forces, the statistical (and, in fact, unknown) nature of the true intermolecular force permits an external force to act as a bias on the otherwise random motion of a solute molecule.

TABLE V
MICROSCOPIC FORCE COMPARISONS IN LIQUIDS*

		Hg	InSb	Na	NH_3	CO_2
INPUT PARAMETERS	ϵ ~ ergs	1.0353×10^{-13}	--	1.898×10^{-13}	7.707×10^{-14}	2.694×10^{-14}
	σ ~ cm	2.827×10^{-8}	--	3.567×10^{-8}	2.9×10^{-8}	3.941×10^{-8}
	r ~ cm	3.59×10^{-8}	--	4.27×10^{-8}	4.3×10^{-8}	5.02×10^{-8}
	m ~ gm	3.33×10^{-22}	1.97×10^{-22}	3.82×10^{-23}	2.82×10^{-23}	7.3×10^{-23}
	χ_2 ~ cm^{-3}	-2.466×10^{-6}	-6.816×10^{-7}	5.859×10^{-7}	--	--
	M_w ~ gm/mole	200.6	116.75	23	--	--
	v ~ cm^3/mole	14.6	18.2	24 6	25	40
	ρ ~ gm/cm^3	13.7	6.43	0.93	--	--
FORCES - DYNES	F_{mol}	8.6×10^{-6}	--	11.6×10^{-6}	3.3×10^{-6}	1.6×10^{-6}
	F_{mag}	1.8×10^{-21}	6.2×10^{-22}	2.34×10^{-18}	--	--
	F_g	3.3×10^{-19}	1.35×10^{-19}	3.74×10^{-20}	2.76×10^{-20}	7.15×10^{-20}

* $\frac{\Delta B}{\Delta X}$ assumed to be 600 $\frac{\text{gauss}}{\text{cm}}$

H assumed to be 60,000 oersteds

2.4 (Continued)

The next step in connecting external fields to solute distribution in the solid is to determine the solute molecule velocity, $\vec{u}$, from the forces acting on the molecule. The practical method of relating velocity to force is through the mobility of the solute molecules

$$\vec{u}(\vec{r},t) = \nu \vec{F}(\vec{r},t) \tag{53}$$

where the term $\vec{F}$ includes all forces acting on the molecule except the random molecular diffusion forces, discussed above, which are included in the mobility, ν. ν depends on diffusion coefficient and temperature which are in turn related to the microscopic fluctuations, both random and oscillatory, of the molecules,[26,27] and therefore to the random intermolecular forces. Thus, for the cases considered here, $\vec{F}$ would be a magnetic or gravitational force (as calculated from equations 46 - 51) while intermolecular forces, such as equation (52), would not appear explicitly in the expression for $\vec{u}$.

The Dependence of Microsegregation on Solute Velocity

Once the velocity of a solute molecule is known in the melt, how does this factor relate to solute distribution in the solid? The following theory, which discusses microsegregation in terms of the stability of the liquid-solid interface, provides a qualitative answer.

Segregation may be divided into two parts: microsegregation and macrosegregation. Microsegregation includes short-range differences in concentration, such as those found between cells, dendrites and grains, while macrosegregation refers to long range variations in composition found along the length of an ingot and between the outside and the center of a casting. The difference in composition between the solid and liquid phases during solidification is responsible for the non-uniform distribution of solute in the final solid alloy.

2.4 (Continued)

The intercellular and interdendritic microsegregation, i.e., the segregation of solute to the cell boundary or inbetween dendritic branches, is the result of lateral diffusion of solute away from the tip of the growing projection. It follows that microsegregation occurs only when the planar solid-liquid interface becomes unstable. Therefore, to study the microsegregation and the substructure of the solute distribution, the morphological stability of the interface separating solid and liquid during solidification needs to be investigated.

Interface instability in crystal growth was first discussed in connection with experiments reported by Rutter and Chalmers[28] in 1953 on the unidirectional crystallization of dilute tin alloys in horizontal boats. They proposed that impurities rejected by the freezing solid can build up ahead of the advancing solid-liquid interface in such a manner that the equilibrium freezing temperature of the liquid adjacent to the solid-liquid interface is above its actual temperature. They postulated that if the "constitutional supercooling" exists, a protuberance on the interface would have a tendency to grow spontaneously, a smooth liquid-solid interface would be unstable and the observed growth forms would result. The conditions under which constitutional supercooling occurs were subsequently placed on a quantitative basis by Tiller, Rutter, Jackson, and Chalmers[29]. The constitutional cooling principle deals with the question of which state, solid or liquid, is thermodynamically favorable in the region of the liquid ahead of the interface and is not based upon the dynamics of the whole system.

A more elegant approach to the stability theory is to consider a small fluctuation on a planar interface and to determine under what conditions the fluctuation decays and under what conditions it grows. This is the perturbation theory of interface stability and has been developed by Wagner[30], Mullins and Sekerka[31,32], Sekerka[33-36] and Voronkov[37]. The perturbation stability theory provides a description of the time evolution of a perturbed interface and the accompanying temperature

2.4 (Continued)

and concentration fields. This description is valid so long as the perturbations and their effects remain sufficiently small to be described by a linear theory. A time and distance scale of perturbed interface phenomena can therefore be ascertained[38].

There are two different but related calculational methods of studying the response of the interface to a perturbation. These are the time-independent and time-dependent stability theories. The time-independent theory[31-33] involves the time implicitly but excludes time as an explicit variable in the description of the temperature and concentration fields. This "steady state" approximation gives valid results for sufficiently slowly growing perturbations. A more complex time-dependent theory has been developed by Sekerka[34] employing time-dependent transport equations. The stability criterion of the time-dependent theory is very complicated and has not been reduced to a practical criterion. To an approximation, the necessary and sufficient condition for interface stability from the time-dependent theory has been found in agreement with that of the time-independent theory. Since the purpose of this study is to determine the effects of external forces on microsegregation of solute atoms during solidification, we have extended the time-independent theory of interface stability[32,33] to include the movement of solute atoms resulting from the external forces which act on them. The stability criteria under different growth conditions are determined, and a method of estimating the size of the substructure is presented.

Let us consider a unidirectional solidification system at constant solidification velocity, V as shown in Figure 12. The coordinate system attached to the planar interface moves with the constant velocity V with respect to the phases of either side. Suppose a sinusoidal ripple of infinitesimal amplitude, δ, with a wavelength

2.4 (Continued)

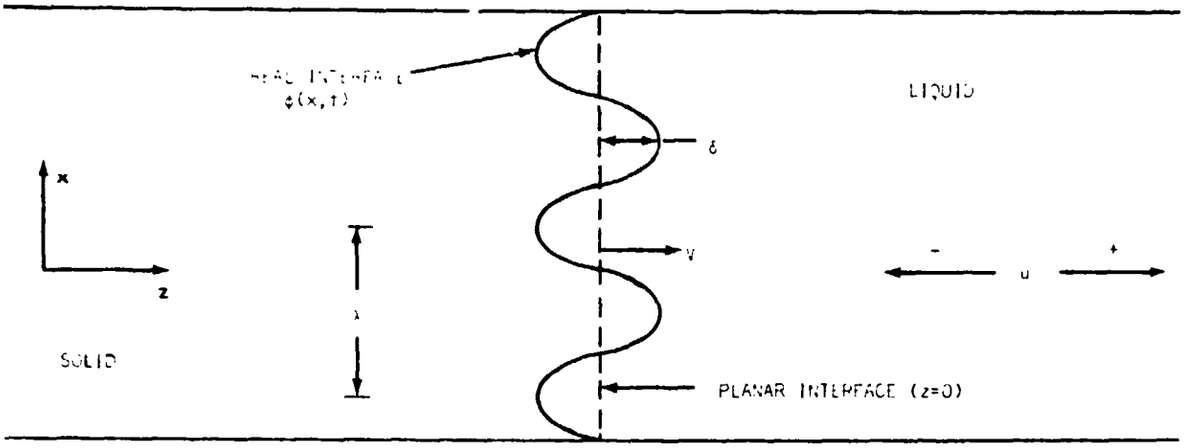

FIGURE 12: INTERFACE GEOMETRY FOR SEKERKA'S THEORY

$\lambda = 2\pi/\omega$ satisfying the relation

$$z = \phi(x,t) = \delta(t) \sin \omega x \tag{54}$$

is introduced into the planar interface between liquid and solid. We wish to obtain an expression for $\dot{\delta} \equiv d\delta/dt$ in order to see whether the ripple grows ($\dot{\delta}>0$) or decays ($\dot{\delta}<0$). This requires us to solve the following simultaneous equations, for the liquid,

$$\nabla^2 C + \frac{1}{D}(V-u)\frac{\partial C}{\partial z} = 0 \tag{55}$$

$$\nabla^2 T + \frac{V}{D_{th}}\frac{\partial T}{\partial z} = 0 \tag{56}$$

and for the solid

$$\nabla^2 T' + \frac{V}{D'_{th}}\frac{\partial T'}{\partial z} = 0 \tag{57}$$

subject to the boundary conditions

$$T_\phi = T'_\phi \tag{58}$$

2.4 (Continued)

$$T_\phi = mC_\phi + T_M + T_M\Gamma\kappa \tag{59}$$

$$= mC_\phi + T_M - T_M\Gamma\delta\omega^2 \sin \omega x$$

$$v(x,t) = \frac{1}{Q}\left[K_s \left(\frac{\partial T'}{\partial z}\right)_\phi - K_L \left(\frac{\partial T}{\partial z}\right)_\phi\right] \tag{60}$$

$$= \frac{1}{C_\phi(k-1)}\left[D \left(\frac{\partial C}{\partial z}\right)_\phi - C_\phi u\right]$$

and to the conditions that for $|\delta|$ much larger than any perturbation on the interface, T, T' and C shall take on the values of the solutions appropriate to the case of a planar interface. The notation is as follows:

$$\nabla^2 = \frac{\partial^2}{\partial x^2} + \frac{\partial^2}{\partial z^2}$$

C = concentration of solute in the liquid

D = solute diffusivity of the liquid (diffusion coefficient)

V = average solidification velocity

u = solute velocity due to external force

T = temperature in the liquid

T' = temperature in the solid

$D_{th} = \frac{K_L}{c_L}$ = thermal diffusivity of the liquid

$D'_{th} = \frac{K_s}{c_s}$ = solid

K_L, K_s = thermal conductivity of the liquid and solid, respectively

c_L, c_s = specific heat per unit volume of the liquid and solid, respectively

m = slope of liquidus line on the phase diagram

T_M = absolute melting point of the pure solvent

Γ = γ/Q, capillary constant

γ = solid-liquid surface free energy

Q = latent heat of fusion of the solvent per unit volume

2.4 (Continued)

κ = average curvature at a point of the interface

$v = V + \frac{d\phi}{dt}$ = interface velocity

k = distribution coefficient = ratio of the equilibrium concentration of solute on the solid side of the interface to that on the liquid side of the interface

subscript ϕ denotes the quantity under consideration is measured at the interface.

Let T_ϕ and C_ϕ be the temperature and concentration at the interface respectively, we have

$$T_\phi = T_o + a\phi = T_o + a\delta \sin \omega x \tag{61a}$$

$$C_\phi = C_o + b\phi = C_o + b\delta \sin \omega x \tag{61b}$$

where T_o and C_o are the values for a flat interface and the second terms are the first-order corrections corresponding to the infinitesimal perturbation. a and b are coefficients to be determined. The solutions of equations (55), (56), and (57) satisfying the condition for large z and reducing to equations (61) on the interface $z = \phi$ are the following:

$$C(x,z) - C_o = \frac{G_c D}{V'} \left[1-\exp\left(\frac{-V'}{D}z\right)\right] + \delta(b-G_c) \sin \omega x \, e^{-\omega^* z} \tag{62a}$$

$$T(x,z) - T_o = \frac{G\, D_{th}}{V} \left[1-\exp\left(\frac{-V}{D_{th}}z\right)\right] + \delta(a-G) \sin \omega x \, e^{-\omega_{th} z} \tag{62b}$$

and on the solid side

$$T'(x,z)-T_o = \frac{G'D'_{th}}{V} \left[1-\exp\left(\frac{-V}{D'_{th}}z\right)\right] + \delta(a-G') \sin \omega x \, e^{-\omega'_{th} z} \tag{62c}$$

where G and G' are the thermal gradients at the unperturbed flat interface (δ=0) in the liquid and solid, respectively, G_c is the concentration gradient in the liquid at the unperturbed flat interface, $V' \equiv V-u$ is the solute velocity relative to that of the interface, and where

2.4 (Continued)

$$\omega^* = \frac{V'}{2D} + \left[\left(\frac{V'}{2D}\right)^2 + \omega^2\right]^{\frac{1}{2}} \tag{63a}$$

$$\omega_{th} = \frac{V}{2D_{th}} + \left[\frac{V}{2D_{th}} + \omega^2\right]^{\frac{1}{2}} \tag{63b}$$

$$\omega'_{th} = -\frac{V}{2D'_{th}} + \left[\frac{V}{2D'_{th}} + \omega^2\right]^{\frac{1}{2}} \tag{63c}$$

Substituting equations (62) into equations (59) and (60), we can determine a and b to the first order in δ. From equations (62) and equation (60), after straightforward but tedious algebra, we have the expression for $\dot{\delta}/\delta$ which is sought

$$\frac{\dot{\delta}}{\delta} = 2\omega\left(V - \frac{u}{p}\right) \frac{mG_c\left(\omega^* - \frac{V'}{D}\right) - \left[T_M\Gamma\omega^2 + \frac{1}{2}(\underline{G}' + \underline{G})\right]\left[\omega^* - \frac{p}{D}\left(V - \frac{u}{p}\right)\right]}{2m\omega L_c + \frac{Q}{K}\left(V - \frac{u}{p}\right)\left[\omega^* - \frac{p}{D}\left(V - \frac{u}{p}\right)\right]} \tag{64}$$

as well as

$$V = \frac{\overline{K}}{Q}(\underline{G}' - \underline{G}) = \frac{1}{Q}(K_s G' - K_L G) \tag{65}$$

$$V = -\frac{DG_c}{pC_o} + \frac{u}{p} \tag{66}$$

where

$\overline{K} = \frac{K_s - K_L}{2}$ = average thermal conductivity of the system

$\underline{G} = \left(\frac{K_L}{\overline{K}}\right)G$ = generalized thermal gradient in the liquid

$\underline{G'} = \left(\frac{K_s}{\overline{K}}\right)G'$ = generalized thermal gradient in the solid

and $p = 1-k$.

Stability of the interface with respect to an undulation depends on the sign of $\dot{\delta}/\delta$; a positive value of $\dot{\delta}/\delta$ for any ω means growth of some undulations and hence instability of the original flat interface

2.4 (Continued)

whereas a negative sign for all ω means decay of all undulations and hence stability. In the present analysis, the conditions $0<k<1$, $m<0$ and G' and $G>0$ are assumed (because these hold true for the usual case). Also, only the condition of $u>0$, i.e., solute atom velocity in the same direction as the solidification velocity, is considered. There are two reasons why $u<0$ is not considered. Physically, $u<0$ means that the solute will pile up at the interface, producing a much more unstable and thus more complicated situation than in the $u>0$ case. Mathematically, when $u<0$, the inequality $V-u > V-\frac{u}{p}$ (which will be utilized presently) does not hold. If this inequality is not valid, the denominator of equation (64) is not necessarily positive, and the stability analysis becomes too complicated to be accomplished within the time frame of the present study. But for the $u>0$ condition. three different cases are analyzed below.

(a) $V - \frac{u}{p} = 0$

From equation (66), we have $V - \frac{u}{p} = -\frac{DG_c}{pC_o}$ which means $G_c \to 0$ and

$$\frac{V - \frac{u}{p}}{G_c} = -\frac{D}{pC_o} \text{ as } V - \frac{u}{p} \to 0.$$ Under this condition, equation (64) becomes

$$\frac{\dot{\delta}}{\delta} = 2\omega \frac{\frac{D}{mpC_o}\left[T_M\Gamma\omega^2 + \frac{1}{2}(G'+G)\right]\omega^*}{2\omega - \frac{Q}{K}\frac{D}{mpC_o}\omega^*}$$

Everything on the right side of the above equation is positive except m which is less than zero. Therefore, we have found, when $V - \frac{u}{p} = 0$, that

$$\frac{\dot{\delta}}{\delta} < 0$$

2.4 (Continued)

which means that the flat interface is always stable under this condition. The physical meaning of $V - \frac{u}{p} = 0$ can be explicitly seen from the following relations. As $V - u/p \to 0$, or $G_c \to 0$, from equation (62) we have $C(x,\infty) = C_o$. This means that the concentration of solute at large distances from the interface is equal to the concentration at the flat interface, or, there is no pile-up of solute at the interface. This condition can be realized by applying a force (such as a magnetic, acceleration or other external force as in equation 53) on the solute atoms in the direction of solidification with a magnitude of

$$F = \frac{1-k}{mQ} (K_s G' - K_L G) \quad . \tag{67}$$

Hence, an external force acting on solute atoms can be expressed in terms of measurable material properties.

(b) $V - \frac{u}{p} > 0$

Under this condition, the following relations may easily be found.

$$V' = V - u > V - \frac{u}{p} > 0 \text{ since } p \equiv 1-k < 1;$$

$$V - \frac{u}{p} = - \frac{DG_c}{pC_o} > 0 \text{ hence } G_c < 0 \text{ and } mG_c > 0;$$

and $$\omega^* = \frac{V'}{D} = \frac{V-u}{D} > \frac{p}{D} (V-u) > \frac{p}{D} (V - \frac{u}{p})$$

With these relations, all terms in the denominator of equation (64) are positive. The sign of $\dot{\delta}/\delta$, or the stability criterion, is solely determined by the sign of the numerator of equation (64) or the sign of $N(\omega)$ which is, from equation (64),

$$N(\omega) = mG_c \left[1 - \frac{\frac{kV}{D}}{\omega^* - \frac{p}{D}(V - \frac{u}{p})}\right] - T_M \Gamma \omega^2 - \frac{1}{2}(\underline{G}' + \underline{G}) \tag{68}$$

$$= f(\omega) - \frac{1}{2}(\underline{G}' + \underline{G}) + mG_c$$

2.4 (Continued)

where

$$f(\omega) = - T_M \Gamma \omega^2 - 2kmG_c \frac{\frac{V}{V'}}{\left[1 + \left(\frac{2D}{V'}\omega\right)^2\right]^{i/2} - 1 + 2k\frac{V}{V'}} \qquad (69)$$

The function $f(\omega)$ has the following properties:

(i) $f(\omega) < 0$.

(ii) $f(0) = -mG_c$ and $f(\infty) = -\infty$

(iii) $f(\omega)$ either decreases monotonically as ω increases from zero or it has only one maximum for some positive value of ω.

Properties (i) and (ii) follow immediately from the expression for $f(\omega)$, equation (69). Property (iii) has been proved in a similar way as in Reference (32). The negativity of $f(\omega)$ means that it always favors stability; evidently it poses the least barrier to instability at the frequency for which it attains its largest value (value of smallest magnitude).

For the case in which $f(\omega)$ decreases monatonically as ω increases from zero so that $|\max f(\omega)| = |f(0)| = mG_c$, the sign of $N(\omega)$ is always negative. Therefore, there can be no instability under this condition. This absolute stability situation occurs when $df/d\omega \leq 0$ for $\omega \to 0$.

For small ω, equation (69) may be expanded in a Taylor's series

$$f(\omega) = -mG_c + \left(\frac{mG_cD^2}{kV'V} - T_M\Gamma\right)\omega^2 + \ldots.$$

then the absolute stability ($df/d\omega \leq 0$ as $\omega \to 0$) occurs when

$$\frac{mG_cD^2}{kV'V} - T_M\Gamma \leq 0$$

or

$$\frac{\left(k\frac{V}{V'}\right) T_M\Gamma V'^2}{mG_cD^2} \geq 1 \qquad (70)$$

2.4 (Continued)

Since, from equation (66)

$$DG_c = -pC_0 \left(V - \frac{u}{P}\right)$$

and from equation (62)

$$C(x,\infty) = C_\infty = C_0 \, k \, \frac{V}{V'} \quad ,$$

the condition of absolute stability (equation 70) in terms of measurable quantities is

$$0 < V - \frac{u}{P} \leq \frac{k^2 T_{M'} V^2}{(-m)\ DpC_\infty} \tag{71}$$

This absolute stability a when, from equation (70),

$$T_{M'} \geq \frac{mG_c D^2}{kV'V}$$

which means that the capillary effect dominates the solute effect.

The old constitutional supercooling criterion[29] is

$$-G+mG_c < 0 \text{ stable} \tag{72a}$$

$$-G+mG_c > 0 \text{ unstable} \tag{72b}$$

Comparing 72b with the criterion of absolute stability (equation 70), we may have a condition that

$$G<mG_c< \frac{kT_{M'}V'V}{D^2} \tag{73}$$

That is, the constitutional supercooling criterion for instability and the condition for absolute stability could be satisfied simultaneously. Hence, according to this theory, the constitutional supercooling is not a sufficient condition to determine the interface stability.

2.4 (Continued)

For the condition that

$$V - \frac{u}{p} > \frac{k^2 T_M \Gamma V^2}{(-m)\ DpC_\infty}$$

or

$$A \equiv \frac{(k\ \frac{V}{V'})\ T_M \Gamma V'^2}{mG_c D^2} = \frac{k^2(\frac{V}{V'})}{1-k(\frac{V}{V'})}\ \frac{T_M \Gamma}{(-m)D}\ \frac{V'}{C_\infty} < 1, \tag{74}$$

the stability criterion is very complicated. The stability conditions will be discussed below using an analytical method similar to that described by Sekerka.[33] From equation (68), the stability criterion is

$$N(\omega) < 0$$

or

$$\frac{\underline{G}' + \underline{G}}{2mG_c} > 1 + \frac{f(\omega)}{mG_c} \tag{75}$$

From equation (69), we have

$$-\frac{f(\omega)}{mG_c} = \frac{T_M \Gamma \omega^2}{mG_c} + \frac{2\ (k\frac{V}{V'})}{[1 + (\frac{2D}{V'}\omega^2)]^{1/2} - 1 + 2\ k\frac{V}{V'}} \tag{76}$$

A new function Y(y) is now defined by

$$Y(y) \equiv -\frac{f(\omega)}{mG_c} = y + \frac{2k'}{(1 + \theta y)^{1/2} - 1 + 2k'} \tag{77}$$

where

$$y = \frac{T_M \Gamma}{mG_c}\omega^2 \geq 0$$

$$k' \equiv k\frac{V}{V'}$$

and $$\theta \equiv \frac{4k'}{A} = \frac{4mG_c D^2}{T_M \Gamma V'^2}$$

2.4 (Continued)

The criterion for a stable interface, from equation (75), becomes

$$\frac{\underline{G}' + \underline{G}}{2mG_c} > 1 - Y(y) \quad . \tag{78}$$

From property (iii) of $f(\omega)$, the $Y(y)$ may have a minimum at a certain value of y. Therefore, the system which is stable for all frequencies has to satisfy the condition

$$\frac{\underline{G}' + \underline{G}}{2mG_c} > S \tag{79}$$

where $S \equiv 1$-[min. $Y(y)$] is defined as the stability function.

To find the value of y at which $Y(y)$ has a minimum, we set

$$\frac{dY(y)}{dy}\Big|_{y=y_m} = 0$$

From equation (77), we have

$$(1 + \theta y_m)^{1/2} = \frac{\theta k'}{[(1 + \theta y_m)^{1/2} - 1 + 2k']^2} \tag{80}$$

Since ω must be real, we have

$$(1 + \theta y_m)^{1/2} - 1 + 2k' > 0$$

and

$$(1 + \theta y_m)^{1/4} > 0$$

By taking the square root of both sides of equation (80), there follows

$$r^2 + (2k' - 1)r - (2k'/A^{1/2}) = 0 \tag{81}$$

where $r = (1 + \theta y_m)^{1/4}$. Since $2k'/A^{1/2} > 0$ and the quadratic term is missing, equation (81) has one and only one positive and real root of r. It is this positive root which corresponds to positive ω. Since

2.4 (Continued)

$$y_m = (r^4-1)\, A/4k' \quad , \tag{82}$$

it follows from the definition of S that

$$S(A,k') = 1-[\min.Y(y)] = 1 + \frac{A}{4k'} - \frac{3A^{1/2}}{2} r - \frac{A(1-2k')}{4k'} r^2 \quad . \tag{83}$$

According to equation (79), stability obtains when

$$\frac{\underline{G}' + \underline{G}}{2mG_c} > S(A,k') \quad . \tag{84}$$

Using equations (65) and (66), the stability condition, equation (84), can be written in terms of experimentally measurable quantities as

$$\frac{2K_L}{K_s+K_L}\left[\frac{G}{V} + \frac{Q}{2K_L}\right] \frac{k'}{1-k'} \frac{D}{(-m)C_\infty} \left(\frac{V}{V'}\right) > S(A,k') \tag{85}$$

If all the material constants, K_L, K_s, Q, k, γ, D and m are specified by a choice of base material and solute, the left hand side of equation (85), defined as a test function, is a function of four variables of operation

$$J\left(\frac{G}{V}, \frac{V}{V'}, C_\infty\right) \equiv \frac{2K_L}{K_s+K_L}\left[\frac{G}{V} + \frac{Q}{2K_L}\right] \frac{k'}{1-k'} \frac{D}{(-m)C_\infty} \left(\frac{V}{V'}\right) \tag{86}$$

Suppressing the explicit appearance of the material constants in the stability function, we call

$$S\left(\frac{V}{V'}, \frac{V'}{C_\infty}\right) = S(A,k') \tag{87}$$

Then for stability, we need the test function to be greater than the stability function, i.e.,

$$J\left(\frac{G}{V}, \frac{V}{V'}, C_\infty\right) > S\left(\frac{V}{V'}, \frac{V'}{C_\infty}\right) \quad . \tag{88}$$

By comparing the stability function, S(A,k') (equation 83), and equation (81) (which we have calculated including the solute atoms moving with velocity u) with Sekerka's stability function, (equations 11 and 14 in Reference 33), the functional form of both functions is seen to be

2.4 (Continued)

identical. Sekerka[33] has calculated his S(A,k) as a function of A in the range $0 \leq A \leq 1$ for 16 values of k. His results are plotted both in linear and semilogarithm scales as shown in Figure 2 and Figure 3 of Reference 33. His results can be directly applied to our results by changing his k and V to $k'(\equiv k\frac{V}{V_T})$ and $V'(\equiv V-u)$.

(c) $V - \frac{u}{p} < 0$

This condition implies, from equation (66), that the solute in the liquid is depleted at the interface ($G_c > 0$) even for $k<1$. It can be easily seen that, from equation (64), $\dot{\delta}/\delta$ is always less than zero if $\underline{G}' + \underline{G}$ is positive. Therefore, the planar interface is a stable condition during the solidification, and microsegregation cannot occur.

It is possible to calculate and plot $\dot{\delta}/\delta$ as a function of frequency ($\omega=2\pi/\lambda$) for any particular experimental case from equation (64). A schematic graph is shown in Figure 13 for a cell growth experiment. It can be seen that within the frequency range, $\omega_1<\omega<\omega_2$, $\dot{\delta}/\delta$ is positive and has a maximum value at ω_m. That is, at $\omega=\omega_m$, the perturbation δ has the fastest growth and the cell size should be dominated by this perturbation. Therefore, we can estimate the order of magnitude of a cell size as $\lambda_m=2\pi/\omega_m$.

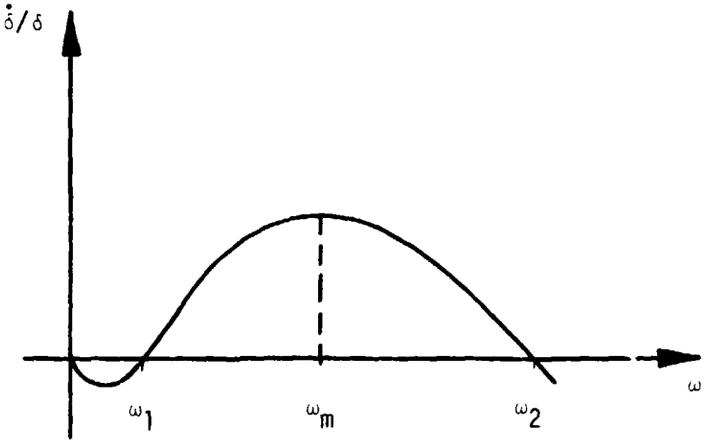

FIGURE 13: $\dot{\delta}/\delta$ VS. ω FOR UNSTABLE INTERFACE CONDITIONS

2.4 (Continued)

As mentioned in Mullins and Sekerka's paper[32], there is no detailed agreement between the theoretically predicted relationship and the experimentally observed relationship of the cell size to the growth parameters. They gave two reasons for this failure: (1) time-independent or steady-state diffusion and temperature fields have been assumed in the calculation, and (2) the cellular structure which develops in actual experiments does not have a small amplitude. The first deficiency of the theory was removed by Sekerka in 1967[34]. He formulated a time-dependent stability theory by using the same small perturbation technique. The results of that theory are very complicated. However, the cell size predicted in a simplified version of the time-dependent theory[35] does still not agree with the observed structure. The main problem is the second failure (above). To remove this obstacle, a finite amplitude theory rather than the small perturbation technique is required. Then the field equations and the boundary conditions all become nonlinear. To date, to our best knowledge, no solution to the nonlinear problem has been achieved.

Thus our theory, which describes an external force field acting on solute atoms, follows a time-independent analysis similar to that of Mullins and Sekerka[32]. We can use the results to estimate the final cell size only to an order of magnitude. We could extend our present theory to a time-dependent theory, but even though such a theory is very complicated, it does not improve the prediction of the final solid substructures.

2.5 REFERENCES

1. R. I. Miller, Analysis of Field Effects on Dense Liquid Materials, NASA CR-124294 (Boeing Document D5-17254) May 9, 1973.

2. R. I. Miller, J. Crystal Growth, 20, 310, 1973.

3. W. R. Smythe, Static and Dynamic Electricity, McGraw-Hill Book Co., New York, 1950.

4. D. Turnbull and M. H. Cohen, J. Chem. Phys., 34, 120, 1961.

5. D. Turnbull and M. H. Cohen, J. Chem. Phys., 52, 3038, 1970.

6. M. H. Cohen and D. Turnbull, J. Chem. Phys., 31, 1164, 1959.

7. M. W. Zemansky, Heat & Thermodynamics, McGraw-Hill Book Co., New York, 1957.

8. D. Turnbull and M. H. Cohen, in Modern Aspects of the Vitreous State, edited by J. D. Mackenzie, Butterworths, Washington, 1960.

9. E. S. Shire, Classical Electricity and Magnetism, Cambridge University Press, 1960.

10. S. Chikazumi and S. Charap, Physics of Magnetism, John Wiley and Sons, New York, 1964.

11. M. Schieber, J. Crystal Growth, 1, 131, 1967.

12. R. Wood, Chemical Thermodynamics, Appleton - Century - Crofts, New York, 1970.

13. V. M. Glazov and S. N. Chizhevskaya, Soviet Physics - Solid State, 6, #6, 1322, 1964.

2.5 (Continued)

14. R. Hultgren. R. L. Orr, P. D. Anderson and K. K. Kelley, Selected Values of Thermodynamic Properties of Metals and Alloys, John Wiley and Sons, New York, 1963.

15. V. I. Davydov, Germanium, Trans. by A. Peiperl, Gordon & Breach, New York, 1966.

16. American Institute of Physics Handbook, 2nd Edition, McGraw-Hill, New York, 1963.

17. R. R. Miller and L. F. Epstein, in Liquid Metals Handbook, edited by C. B. Jackson, U.S.A.E.C. and Bureau of Ships, Department of the Navy, 1955.

18. E. W. Washburn, Ed., International Critical Tables, 6, McGraw-Hill, New York, 1929.

19. R. Dupree and E.F.W. Seymour in Liquid Metals - Chemistry and Physics, edited by S. Z. Beer, Marcel Dekker, New York, 1972.

20. R. I. Miller, Metallurgical Transactions, 5, 643, 1974.

21. J. D. Jackson, Classical Electrodynamics, John Wiley and Sons, New York, 1965.

22. M. Caputo, The Gravity Field of the Earth, Academic Press, New York, 1967.

23. C. A. Wert and R. M. Thomson, Physics of Solids, McGraw-Hill Book Co., New York, 1964.

24. C. Kittel, Introduction to Solid State Physics, 3rd Edition, John Wiley and Sons, New York, 1967.

2.5 (Continued)

25. J. A. Pryde, The Liquid State, Hutchinson & Co., London, 1966.

26. P. A. Egelstaff, An Introduction to the Liquid State, Academic Press, London, 1967.

27. K. Huang, Statistical Mechanics, John Wiley and Sons, New York, 1967.

28. J. W. Rutter and B. Chalmers, Can. J. Phys., 31, 15, 1953.

29. W. A. Tiller, J. W. Rutter, K. A. Jackson and B. Chalmers, Acta. Met., 1, 428, 1953.

30. C. Wagner, J. Electrochem. Soc.,103, 571, 1956.

31. W. W. Mullins and R. F. Sekerka, J. Appl. Phys., 34, 323, 1963.

32. W. W. Mullins and R. F. Sekerka, J. Appl. Phys., 35, 444, 1964.

33. R. F. Sekerka, J. Appl. Phys., 36, 264, 1965.

34. R. F. Sekerka, J. Phys. Chem. Solids, Supplement 1, 691, 1967.

35. R. F. Sekerka, J. Phys. Chem. Solids, 28, 983, 1967.

36. R. F. Sekerka, Crystal Growth, Ed. H.S. Peiser, Pergamon, 1967.

37. V. V. Voronkov, Sov. Phys.-Solid State, 6, 2378, 1965.

38. R. F. Sekerka, J. Crystal Growth, 3,4, 71, 1968.

2.5 (Continued)

39. V. M. Glazov, S. N. Chizhevskaya and N. N. Glagoleva, Liquid Semiconductors, Plenum Press, New York, 1969.

40. V. F. Sears, Proc. Phys. Soc., 86, 953, 1965.

APPENDIX A

SUMMARY OF PUBLICATIONS AND PRESENTATIONS PRODUCED UNDER CONTRACT NAS8-28664

PUBLICATIONS

1. A Summary of Liquid State Models for Materials Processing in Space, Boeing Document D5-17268, August 1972.

2. Analysis of Field Effects on Dense Liquid Materials, NASA CR-124294, May 1973.

3. "Qualitative Effects of Oscillatory Fields on Crystal Melts", Journal of Crystal Growth, 20, 310, November 1973.

4. "Thermodynamic Properties Derived From the Free Volume Model of Liquids", Metallurgical Transactions, 5, 643, March 1974.

5. Further Analysis of Field Effects on Liquids and Solidification, Boeing Document D256-10024, July 1974.

6. "External Field Effects on Solidification: Macroscopic and Microscopic Models", Proceedings of the 1974 AIAA/ASME Thermophysics and Heat Transfer Conference, July 1974.

7. "External Field Effects on Diffusion and Solidification Derived from the Free Volume Model", Submitted to Journal of Applied Physics.

PRESENTATIONS

1. "The Free Volume Model Equation of State", Annual Meeting of SESAPS*, November 1972.

2. "External Field Effects on Solidification Rate", Annual Meeting of SESAPS*, November 1973.

APPENDIX A (Continued)

3. "Some Aspects of Present and Future Research in Space" (Invited Paper), Annual Meeting of SESAPS*, November 1973.

4. "External Field Effects on Solidification: Macroscopic and Microscopic Models" AIAA/ASME Thermophysics and Heat Transfer Conference, July 1974.

*Southeast Section of the American Physical Society

APPENDIX B

BOUNDARY CONDITIONS ON MAGNETIC FIELDS FOR THE CASE OF CZOCHRALSKI CRYSTAL GROWTH GEOMETRY

From the Maxwell equation for the divergence of the magnetic induction field, $\vec{\nabla}\cdot\vec{B} = 0$, it can be shown[21] that the normal component of $\vec{B}$ must be continuous across each boundary, or

$$(\vec{B}_2 - \vec{B}_1) \cdot \hat{n} = 0 \tag{B-1}$$

where $\hat{n}$ is a unit vector normal to the surface. Since

$$\vec{B} = \mu\vec{H} = -\mu\vec{\nabla}\phi \tag{B-2}$$

this condition implies that

$$\mu_1 \vec{\nabla}\phi_1 = \mu_2 \vec{\nabla}\phi_2 \tag{B-3}$$

For this condition to hold, it is obvious that the potential, ϕ, must itself be continuous across a boundary

$$\phi_1 = \phi_2 \tag{B-4}$$

and to insure physically reasonable results, we must impose the conditions that ϕ be finite everywhere and that at distances far from the boundaries of interest, the field approach the value the field would have if there were no material boundaries present.

The following boundary conditions are based on the above principles, and the assumption that the cylindrical geometry is divided into four regions as shown in Figure B-1, even though regions 3 and 4 are physically identical.

$$\phi_1 (0,\theta,-\infty),\ \phi_2 (0,\theta,+\infty) = \text{finite} \tag{B-5}$$

$$\phi(r,\theta,z) \xrightarrow[r \to \infty]{} - H_0 r \cos\theta \tag{B-6}$$

APPENDIX B (Continued)

$$\phi_3(a,\theta,z) = \phi_1(a,\theta,z) \tag{B-7}$$

$$\mu_0 \frac{\partial \phi_3}{\partial r}\Big|_a = \mu_1 \frac{\partial \phi_1}{\partial r}\Big|_a \tag{B-8}$$

$$\phi_4(b,\theta,z) = \phi_2(b,\theta,z) \tag{B-9}$$

$$\mu_0 \frac{\partial \phi_4}{\partial r}\Big|_b = \mu_2 \frac{\partial \phi_2}{\partial r}\Big|_b \tag{B-10}$$

$$\phi_4(r,\theta,0) = \phi_1(r,\theta,0), \quad b<r<a \tag{B-11}$$

$$\mu_0 \frac{\partial \phi_4}{\partial z}\Big|_0 = \mu_1 \frac{\partial \phi_1}{\partial z}\Big|_0, \quad b<r<a \tag{B-12}$$

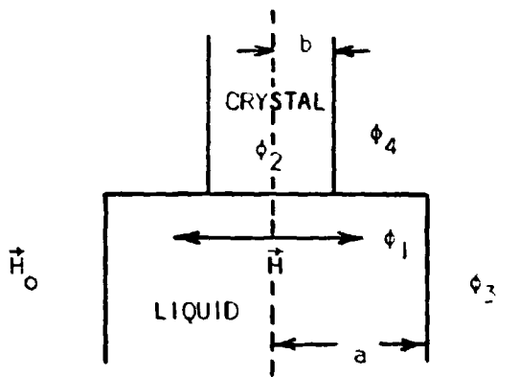

FIGURE B-1: CZOCHRALSKI GEOMETRY FOR MAGNETIC POTENTIALS

APPENDIX C
MAGNETIC FIELD FORCES ON MOVING CHARGED MOLECULES IN A MELT

A molecule which possesses a net electric charge, q, and which is in motion relative to magnetic field lines in a melt will experience Lorentz forces just as will any charged particle moving in a magnetic field. The evidence that particles in melts of semiconductor materials are charged is stated by Glazov, et.al.[39], who suggest that in many such melts, q = 4e where e is the electron charge. Thus the Lorentz force on the molecule is

$$\vec{F}_L = q\,\vec{u} \times \vec{B} \tag{C-1}$$

where

$$\vec{u} = \vec{u}_0 + \vec{u}_t \tag{C-2}$$

with $\vec{u}_0$ being an scillatory velocity, $\dot{\vec{r}}_0$, about some center of vibration, $\vec{r}$, which moves through the melt with the translational velocity, $\vec{u}_t = \dot{\vec{r}}_t$. The situation is represented schematically in Figure C-1.

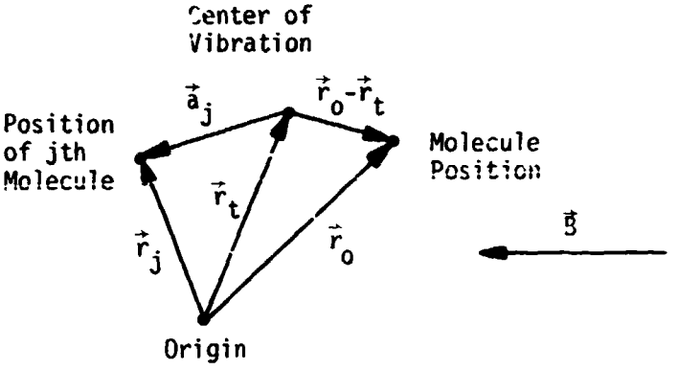

FIGURE C-1: ITINERANT OSCILLATOR GEOMETRY

The velocities $\vec{u}_0$ and $\vec{u}_t$ may be obtained formally from the Itinerant Oscillator model[46]. This model is based on the solution of the two coupled acceleration equations

$$\ddot{\vec{r}}_0 + \eta_0 \dot{\vec{r}}_o + \omega_0^2 (\vec{r}_0 - \vec{r}_t) = \vec{A} \tag{C-3}$$

APPENDIX C (Continued)

$$\ddot{\vec{r}}_t + \gamma_t \dot{\vec{r}}_t = \vec{D} \qquad \text{(C-4)}$$

where γ_0 and γ_t are friction constants, ω_0 is the oscillation frequency which is related to the intermolecular forces acting on the molecule, $\vec{A}$ is a randomly fluctuating driving acceleration also related to intermolecular forces (and thus distances, $\vec{a}_j$) and the term $\vec{D}$ contains the random Brownian motion-type acceleration and, after the magnetic field has been applied for some time greater than the initial transient (or build-up) period, also contains accelerations arising from the Lorentz force, equation C-1. Accelerations derived from the oscillatory motions should have a net time averaged value of zero. $\vec{D}$ must also include accelerations due to electrostatic forces between charged molecules.

A more detailed analysis of magnetic forces on moving charged molecules in a melt is beyond the scope of this study, since such an analysis simultaneously involves two extremely difficult problems. Although the Lorentz force itself is well understood, actually calculating trajectories and velocities for particles which the force affects and which are moving through a medium other than vacuum is not so simple. The description of molecular motion (diffusion), is reasonably well understood on a statistical or macroscopic basis (see sections 2.3 and 2.4), but on a microscopic basis, the motion of an individual molecule in the absence of external forces depends on random processes which are difficult to describe mathematically.

Thus even though the Itinerant Oscillator model may provide a formal relation between Lorentz forces and charged particle motion in a melt, much more theoretical effort is required in order to determine the real nature of $\vec{F}_L$ in melts of semiconductors.